Journal of Structural Geology 109 (2018) 99–119

Contents lists available at ScienceDirect

Journal of Structural Geology

journal homepage: www.elsevier.com/locate/jsg

Distinguishing thrust sequences in gravity-driven fold and thrust belts

G.I. Alsop[a,*], R. Weinberger[b,c], S. Marco[d]

[a] Department of Geology and Petroleum Geology, School of Geosciences, University of Aberdeen, Aberdeen, UK
[b] Geological Survey of Israel, Jerusalem, Israel
[c] Department of Geological and Environmental Sciences, Ben Gurion University of the Negev, Beer Sheva, Israel
[d] Department of Geophysics, School of Geosciences, Tel Aviv University, Israel

ARTICLE INFO

Keywords:
Thrust
Overstep
Piggyback
MTD
Soft sediment
Dead sea

ABSTRACT

Piggyback or foreland-propagating thrust sequences, where younger thrusts develop in the footwalls of existing thrusts, are generally assumed to be the typical order of thrust development in most orogenic settings. However, overstep or 'break-back' sequences, where later thrusts develop above and in the hangingwalls of earlier thrusts, may potentially form during cessation of movement in gravity-driven mass transport deposits (MTDs). In this study, we provide a detailed outcrop-based analysis of such an overstep thrust sequence developed in an MTD in the southern Dead Sea Basin. Evidence that may be used to discriminate overstep thrusting from piggyback thrust sequences within the gravity-driven fold and thrust belt includes upright folds and forethrusts that are cut by younger overlying thrusts. Backthrusts form ideal markers that are also clearly offset and cut by overlying younger forethrusts. Portions of the basal detachment to the thrust system are folded and locally imbricated in footwall synclines below forethrust ramps, and these geometries also support an overstep sequence. However, new 'short-cut' basal detachments develop below these synclines, indicating that movement continued on the basal detachment rather than it being abandoned as in classic overstep sequences. Further evidence for 'synchronous thrusting', where movement on more than one thrust occurs at the same time, is provided by displacement patterns on sequences of thrust ramp imbricates that systematically increases downslope towards the toe of the MTD. Older thrusts that initiate downslope in the broadly overstep sequence continue to move and therefore accrue greater displacements during synchronous thrusting. Our study provides a template to help distinguish different thrust sequences in both orogenic settings and gravity-driven surficial systems, with displacement patterns potentially being imaged in seismic sections across offshore MTDs.

1. Introduction

Piggyback or foreland-propagating thrust sequences, where younger thrust imbricates develop in the footwalls of existing thrusts, are generally assumed to be the typical order of thrust development in most tectonic settings (e.g. Boyer and Elliot, 1982; Morley, 1988; Fossen, 2016, p.359). However, Boyer (1992, p. 377) notes that such foreland-propagating systems "have taken on the role of an axiom in the study of thrust kinematics" while Butler (2004, p.2) challenges "the dogma of simple foreland-propagation". An alternative overstep thrust sequence, where later thrusts develop in the hangingwalls of earlier thrusts, may also develop (e.g. Elliot and Johnson, 1980, p. 90; Boyer and Elliot, 1982; Park, 2013, p.16). Such overstep thrust sequences are considered to be particularly relevant to gravity-driven mass transport deposits (MTDs), where retrogressive slope failure encourages the locus of deformation to migrate upslope, while thrusting is still directed downslope. Overstep thrust sequences have been interpreted to develop during cessation of movement in MTDs for more than 30 years since the application of the 'dislocation model' to slumps by Farrell (1984), but no outcrop detail has been provided (see Farrell, 1984; Martinsen and Bakken, 1990).

Suggestions of overstep thrust sequences imaged in seismic data from the offshore Norwegian margin were described by Ireland et al. (2011, p. 34) who noted that "Thrusts probably propagated retrogressively based upon the observation that fold amplitudes decrease upslope". Working with seismic sections from the Orange Basin of offshore Namibia, de Vera et al. (2010, p.230) also suggested that local areas of overstep thrusting develop due to truncation of underlying structures by overlying thrusts, although an overall piggyback system of thrusting is considered to operate. In a further seismic example across a fold and thrust system developed offshore Borneo, Totake et al. (2017) recognised that "upper imbricate sheets appear to be younger than underlying sheets, creating a similar structure to break-backward imbricate structure" (i.e. overstep thrusting).

* Corresponding author.
E-mail address: Ian.Alsop@abdn.ac.uk (G.I. Alsop).

https://doi.org/10.1016/j.jsg.2018.01.005
Received 13 June 2017; Received in revised form 15 January 2018; Accepted 22 January 2018

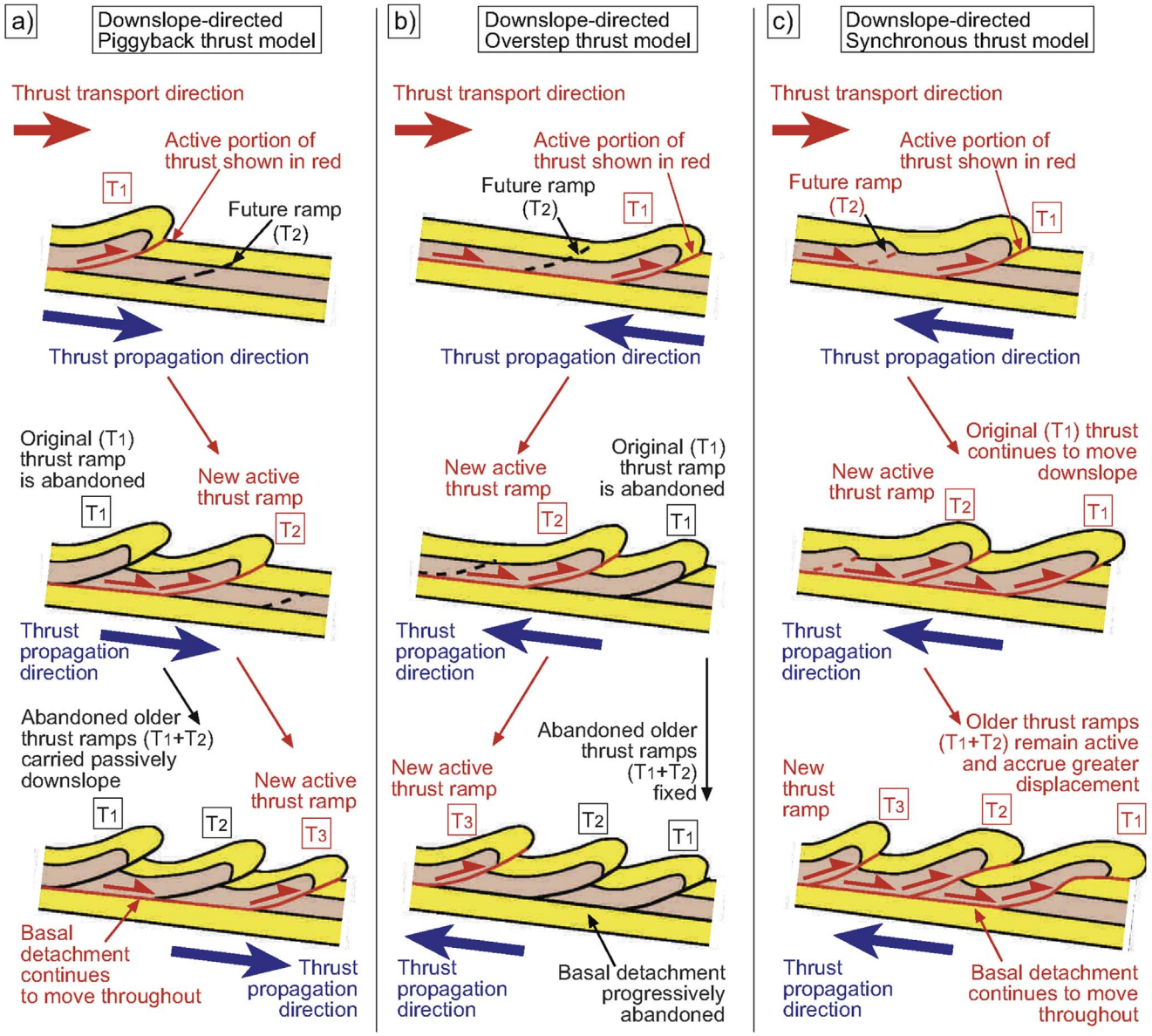

Fig. 1. Schematic illustrations of sections across a) piggyback, b) overstep and c) synchronous thrust sequences in a downslope-directed mass transport deposit (MTD). In c), a thrust system that initiates in an overstep sequence subsequently undergoes continued synchronous thrusting. In each case, thrusts (T) are numbered in the order of development (T1, T2, etc.) and are shown in red where active and black where inactive, while the direction of thrust transport (large red arrow) and overall thrust propagation (blue arrow) are also highlighted. (For interpretation of the references to colour in this figure legend, the reader is referred to the Web version of this article.)

Gross age relationships of gravity-driven fold and thrust belts may be discernible on seismic sections where the ages of strata within, and overlying, an MTD may be determined (e.g. Bull et al., 2009; Morley et al., 2011; Peel, 2014; Reis et al., 2016; Cruciani et al., 2017). Overlying strata that display onlap relationships onto structures and bathymetry created by the MTD are particularly useful in bracketing the timing of thrust movement (e.g. Frey-Martinez et al., 2005; Jolly et al., 2016; Scarselli et al., 2016). A number of seismic studies tentatively interpret piggyback sequences within gravity-driven fold and thrust belts based on "increasing (thrust) dips back up the regional slope" (de Vera et al., 2010, p.229), or " back rotation and straightening of inner, older thrust ramps" (Scarselli et al., 2016, p.168), with older thrusts considered to be steepened-up by new thrusts forming in their footwall. However, despite improvements in seismic imaging, the resolution still does not typically permit detailed cross-cutting relationships between individual thrusts and folds within imbricate sequences to be clearly determined. Indeed, some authors stress that numbering of thrusts on seismic sections does "not imply a sequence of formation" (Butler and Paton, 2010, p.7), while Frey-Martinez et al. (2006, p.591) stress that it is not possible to give a definitive direction of thrust propagation. Thus, within many natural gravity-driven systems associated with MTDs, there remains significant uncertainty as to the order of development of thrust sequences.

Field-based studies of ancient MTDs may provide further information about styles of deformation (e.g. Woodcock, 1976a, b; 1979; Ortner and Kilian, 2016; Korneva et al., 2016) and the sequence of thrust development (e.g. Lucente and Pini, 2003; Sharman et al., 2015; Sobiesiak et al., 2017), although they may be complicated by the effects of later regional tectonism that frequently masks original relationships generated during MTD emplacement. In addition, although such outcrop-based work enables small-scale details to be ascertained (e.g. Gibert et al., 2005; Garcia-Tortosa et al., 2011; Basilone, 2017), it is sometimes limited by the nature and extent of good exposures, with Ireland et al. (2011, p 34) noting only "rare opportunities to study the geometry of internal deformation (within) submarine landslides". Martinsen and Bakken (1990, p.162) examined onshore exposures of Carboniferous

age slumps in western Ireland and note that the truncation of underlying structures by overlying thrusts "suggest that the compressional zone developed in an overstep manner". They concluded that in the downslope (toe) regions of MTDs, the "development of thrusts in an overstep manner rather than in a piggyback fashion may be the expected" (Martinsen and Bakken, 1990, p.163).

In order to investigate detailed thrust sequences within gravity-driven fold and thrust belts, and the potential role that overstep thrust sequences may play, we have therefore undertaken an outcrop-based analysis of relatively recent (< 70 ka) thrust sequences developed in an MTD in the southern Dead Sea Basin. Superb exposure allows cross-cutting relationships and hence timing of thrust sequences to be directly determined, and enables the following fundamental research questions to be addressed.

i) What criteria can be used to distinguish different thrust sequences?
ii) What are the cross-cutting relationships between forethrusts and backthrusts?
iii) Why do overstep thrust sequences develop?
iv) Can some thrusts move synchronously?
v) How do displacement-distance plots relate to overstep thrust sequences?
vi) Which models best constrain the geometry and kinematics of MTDs?

2. Thrust sequences

A variety of different thrust sequences can theoretically be applied to orogenic belts and gravity-driven fold and thrust systems that form MTDs.

2.1. Piggyback thrust sequences

Where new thrusts develop in the footwall of older thrusts, the older thrust is displaced by movement on the younger thrust in a 'piggyback' or foreland-propagating thrust sequence (e.g. Dahlstrom, 1970, p. 349; Butler, 1982, p. 240, his Fig. 4) (Fig. 1a). In a sequence of thrusts, this behaviour results in higher thrusts representing the earliest displacement, while the lowermost thrusts contain the youngest movement (e.g. Dahlstrom, 1970, p.354; Cooper, 1981, p. 228; Butler, 1982, 1987, p.240, p. 620, his Fig. 2). The basal detachment is considered to be active throughout translation of the thrust sheet, resulting in older thrust ramps (T1) being passively carried in its hangingwall (Fig. 1a). Overall, the thrust system therefore propagates in the transport direction, which in orogenic belts is towards the foreland, whereas in gravity-driven MTDs is downslope broadly towards the depocentre of the basin (Fig. 1a).

2.2. Overstep thrust sequences

Where new thrusts develop in the hangingwall of older thrusts, an 'overstep' (or 'break-back') thrust sequence develops (e.g. Elliot and Johnson, 1980, p.90; Boyer and Elliot, 1982, p.1209; Butler, 1982, p. 240) (Fig. 1b). In a sequence of thrusts, this behaviour results in higher thrusts representing the youngest displacement, while the lowermost thrusts contain the earliest movement (e.g. Butler, 1982, p.240, his Fig. 5). In strict overstep thrusting, the basal detachment formed during translation of the thrust sheet, would become progressively inactive from the foreland (toe) as deformation migrated back towards the hinterland (upslope in MTDs) (Fig. 1b). Consequently, older thrusts (T1) maintain a fixed position on the slope once abandoned (Fig. 1b). Overall, the thrust system therefore propagates in a direction opposite to the transport direction, which in orogenic belts is towards the hinterland, whereas in gravity-driven MTDs is upslope away from the depocentre of the basin (Fig. 1b).

2.3. Synchronous thrust sequences

Synchronous thrusting may simply be defined as "when two or more thrusts move together" (McClay, 1992, p.431) and has been applied to a number of orogenic thrust belts (e.g. Morley, 1988; Boyer, 1992; Butler, 2004) and gravity-driven MTDs (e.g. Cruciani et al., 2017) (Fig. 1c). Imbricates within a synchronous thrust system may still initiate in a systematic order, with older thrusts that propagate downslope in a piggyback sequence, or thrusts getting younger upslope in an overstep sequence (see Sections 2.1. and 2.2. above). Within synchronous thrusts systems, the earlier formed thrusts (T1) remain active, even when younger thrusts (T2) are moving, thereby leading to older thrusts accruing the greater displacements (Boyer, 1992), (Fig. 1c). Within MTDs, this behaviour results in older thrusts (T1) being carried downslope by the underlying basal detachment that continues to move (Fig. 1c). Thus, during synchronous thrusting of broadly overstep sequences, the final position of thrust imbricates is not fixed and is dependent on both the rate of thrust slip downslope and the rate of upslope propagation of new thrusts (Fig. 1c).

3. Geological setting

The Dead Sea Basin is a pull-apart basin developed between two left-stepping, parallel fault strands that define the sinistral Dead Sea Fault (Garfunkel, 1981; Garfunkel and Ben-Avraham, 1996) (Fig. 2a and b). The Dead Sea Fault has been active since the Early to Middle Miocene (e.g. Bartov et al., 1980; Nuriel et al., 2017) including during deposition of the Lisan Formation in Lake Lisan that covered up to ~2000 km^2 in the late Pleistocene (70-15 ka) (Haase-Schramm et al., 2004). This fault produced numerous earthquakes triggering co-seismic deformation (e.g. Agnon et al., 2006; Weinberger et al., 2016) as well as soft-sediment deformation and slumping in the Lisan Formation (e.g. El-Isa and Mustafa, 1986; Marco et al., 1996; Alsop and Marco, 2011, 2014; Alsop et al., 2016). The slump systems around the Dead Sea Basin are developed on very gentle slopes of < 1° dip and define an overall regional pattern of radial slumping associated with MTDs that are directed towards the depo-centre of the present Dead Sea Basin (Alsop and Marco, 2012a, 2013). Such a coherent pattern indicates that the slopes were original and linked to the basin depo-centre rather than wholesale later tectonic tilting. The observation that MTDs on the eastern side of the Dead Sea are transported towards the west (El-Isa and Mustafa, 1986) and the centre of the basin also supports the original palaeoslope interpretation. The investigation of drill cores taken from the depo-centre of the Dead Sea reveals that the stratigraphic thickness of the Lisan Formation is three times greater than its onshore equivalent, largely due to the input of MTDs from around the basin margin that 'pond' and accumulate in the depo-centre. (Marco and Kagan, 2014; Lu et al., 2017).

The Lisan Formation comprises a sequence of alternating aragonite-rich and detrital-rich laminae on a sub-mm scale. They are thought to represent annual varve-like cycles with aragonite-rich laminae precipitating from hypersaline waters in the hot dry summer, while winter flood events wash clastic material into the lake to form the detrital-rich laminae (Begin et al., 1974). Varve counting combined with isotopic dating suggests that the average sedimentation rate of the Lisan Formation is ~1 mm per year (Prasad et al., 2009). Detrital laminae within the varved aragonite-rich Lisan Formation display grain sizes of ~8–10 μm (silt), while the thicker detrital-rich units are generally coarser grained (60–70 μm) and can be classified as very fine sands (Haliva-Cohen et al., 2012). Compositionally, the detrital units mainly consist of quartz and calcite grains with minor feldspar, and clays (illite-smectite) (Haliva-Cohen et al., 2012). Seismic events along the Dead Sea Fault are considered to trigger surficial slumps within the Lisan Formation (Marco and Agnon, 1995; Lu et al., 2017), resulting in well-developed gravity-driven fold and thrust belts in the MTDs (Alsop and Marco, 2011; Alsop et al., 2017a). Individual slump sheets are

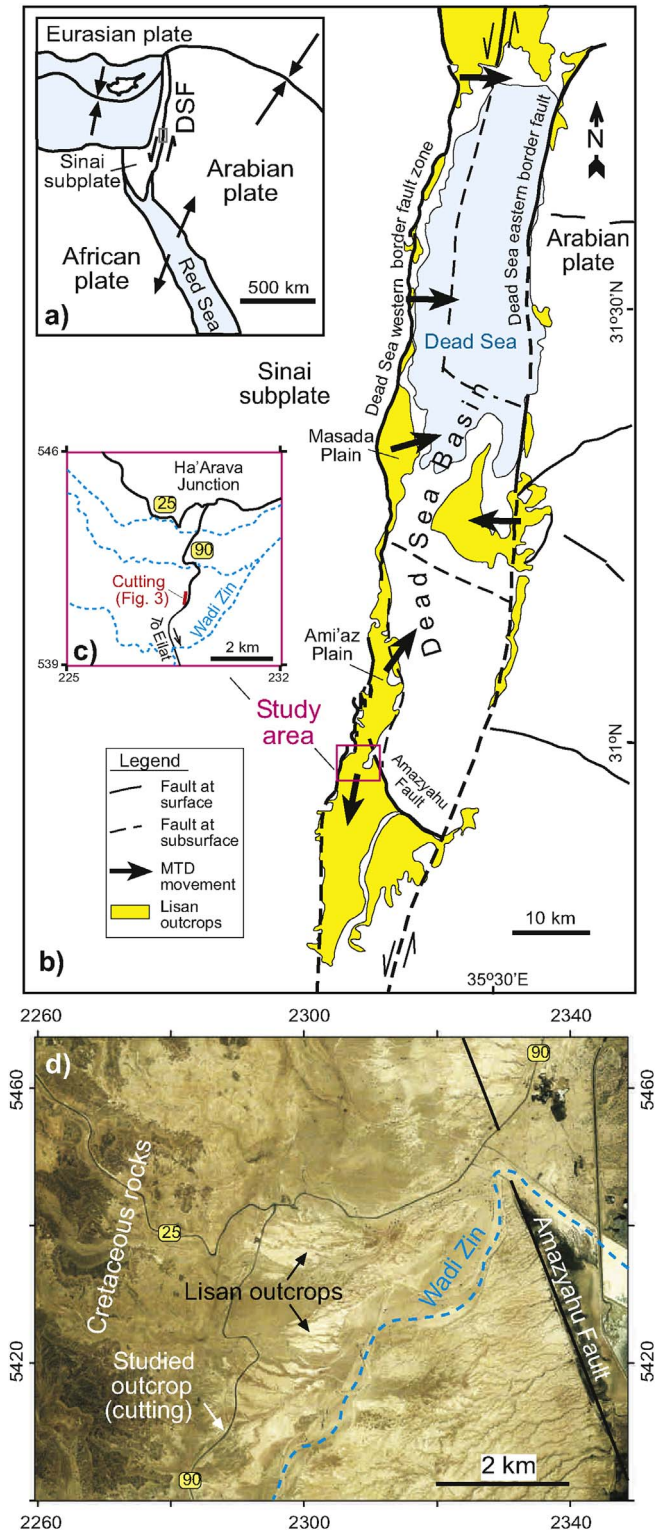

Fig. 2. a) Tectonic plates in the Middle East. General tectonic map showing the location of the present Dead Sea Fault (DSF). b) Map of the current Dead Sea showing the position of the Wadi Zin case study area (red box) (based on Sneh and Weinberger, 2014). c) Inset locality map showing details of the Zin case study area and location of the cutting (Fig. 3) relative to major Highways 25 and 90. d) Image of the light-coloured Lisan Formation at Wadi Zin, with the brownish Cretaceous rocks to the west and the trace of the Amazyahu Fault to the east. Coordinates of the Israel national grid are shown. (For interpretation of the references to colour in this figure legend, the reader is referred to the Web version of this article.)

typically < 1.5 m thick and are capped by undeformed horizontal beds of the Lisan Formation, indicating that fold and thrust systems formed at the sediment surface, with the position of basal detachments controlled by variable lithologies and potentially fluid pressure (e.g. Alsop et al., 2016, 2017a).

The Zin case study area (N30°57′38″ E35°18′9″) is located to the NW of Wadi Zin, which is positioned between the Dead Sea western border fault zone, which bounds the Cretaceous basin margin ~1 km to the west, and the Amazyahu Fault ~ 5 km further NE (Fig. 2b, c, d). This area is ideal for the present case study concerning thrust sequences in unlithified sediments of MTDs as it is well exposed and accessible along cuttings. The varved lacustrine sequence permits high resolution mm-scale correlation of sequences across thrust faults. In addition, the nature of the surficial slumping, where overburden has not exceeded a few metres (e.g. Alsop et al., 2016), removes many complications associated with changes in geometries and angles arising from subsequent compaction of sediments. The Lisan Formation is considered to have been fluid-saturated at the time of deformation, with numerous fluidised clastic dykes cutting the deformed beds (see Alsop et al., 2017c), while the present fluid content is still ~ 25% (Arkin and Michaeli, 1986; Frydman et al., 2008). The actual water depth in the lake has been discussed in detail by Alsop and Marco (2012b) who suggest that sediments were below storm wave base, with water likely to have been between 30 m and 100 m deep at the time of deformation.

4. Orientation and vergence of the fold and thrust system

The Zin case study area (N30°57′38″ E35°18′9″ or N31.00615, E35.26342) contains a number of natural outcrops immediately to the west of Highway 90 that runs south to Eilat (Fig. 2c and d, 3a). In general, folds and thrusts within the Lisan Formation verge predominantly towards the south throughout this area (Fig. 3a). There are also a number of sub-ordinate south-dipping and north-verging backthrusts that are generally steeper and are similar to backthrusts seen elsewhere in the Lisan Formation (Fig. 3a) (e.g. Alsop et al., 2017b). The area is dominated by these contractional structures that we interpret to verge down slope (e.g. Alsop and Marco, 2012a; Alsop et al., 2016).

The main basal detachment to the fold and thrust system is developed a few mm below a distinctive 5 cm thick dark green detrital-rich layer that forms a prominent marker in the sequence (Figs. 3a and 4a). The thrust sequence overlying the basal detachment is 80–100 cm thick, suggesting that the detachment formed about 1 m below the lake floor, and is therefore similar in thickness to other deformed units in the Lisan Formation (Alsop et al., 2016). The MTD horizon is overlain by an undeformed depositional cap that varies in thickness, but is typically less than 10 cm (Fig. 4a, c, e, g). The cap, that comprises detritals and mm-scale aragonite fragments, is interpreted to have been deposited out of suspension following downslope movement of the MTD (see Alsop and Marco, 2012b).

In addition to the general outcrops, a N-S (020°–200°) trending cutting adjacent to a disused track approximately 30 m west of Highway 90 provides a superb section along an imbricated fold and thrust sequence (Fig. 2c and d, 3b, c). The 25 m long cutting contains 7 north-dipping forethrust ramps (FT) that are directed towards the south, and also three steeper backthrusts (BT) verging northwards (Figs. 3b, c, 4a–h). Associated fold hinges are E-W trending and sub-horizontal, with the fold hinges and axial planes trending broadly parallel to the strike of the related thrust planes (Figs. 3d, 4a–h). The normals to the mean thrust strike and mean fold axes are towards 194° and 181°, respectively (Fig. 3d). Individual thrusts and folds follow this overall transport direction, with thrust transport directions ranging from 181° to 208°, while transport calculated from the normal to fold hinges vary from 182° to 204° (see Alsop and Marco, 2012a; Alsop et al., 2016 for methodologies of determining MTD movement) (Fig. 4a–h). The 220° trending section is therefore almost transport-

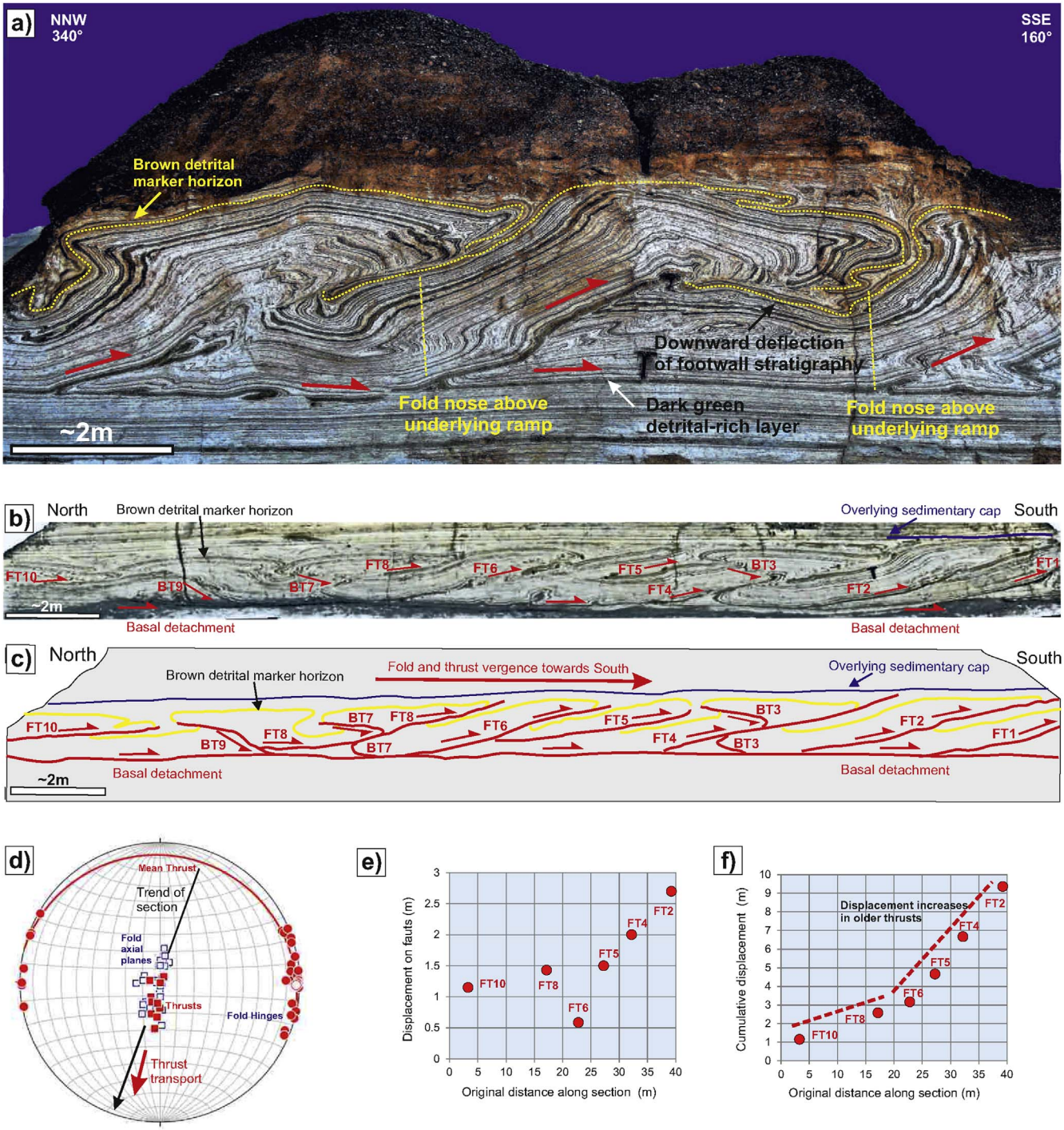

Fig. 3. a) Imbricated south-verging thrusts and associated folds developed within the Lisan Fm. at Wadi Zin (N30°57′38″ E35°18′9″). The photograph has been mirrored so that south is uniformly towards the right-hand side of all photos. b) View of the imbricated sequence along a disused track, while c) shows an interpretation of the same section with the basal detachment displaying forethrust ramps (FT) and backthrusts (BT) that are sequentially numbered from oldest (1) to youngest (10). A distinctive 10 cm thick detrital marker horizon is highlighted (in yellow), while a sedimentary capping layer deposited from suspension following the slump is shown in blue. d) Stereonet of thrust planes (N = 11), and folds (N = 32), showing fold hinges (mean 3/091), axial planes (N = 29) and thrust planes (mean 104/10N). Structural data on the stereonet is represented as follows: fold hinges (solid red circles), mean fold hinge (open red circle), poles to fold axial planes (open blue squares), thrust planes (red great circles), and poles to thrust planes (solid red squares). Calculated slump transport directions based on thrust data (red arrow) are subparallel to the trend of the outcrop section (black arrows). e, f) Graphs comparing the original distance along the section (measured from the northern end) with e) displacement on each forethrust (FT), and f) cumulative displacement on the forethrust sequence. (For interpretation of the references to colour in this figure legend, the reader is referred to the Web version of this article.)

parallel and suitably orientated for structural analysis.

4.1. Overall displacement patterns along an imbricate section

A 7 cm thick, dark brown detrital-rich bed towards the top of the sequence forms a clear marker horizon (highlighted in yellow on Fig. 3b and c) that may be readily traced around folds and across thrusts. Restoration of this marker suggests ~40% shortening along the section, which is a similar value to other restored thrust sections in the Lisan Formation (e.g., Alsop et al., 2017a). In detail, the amount of

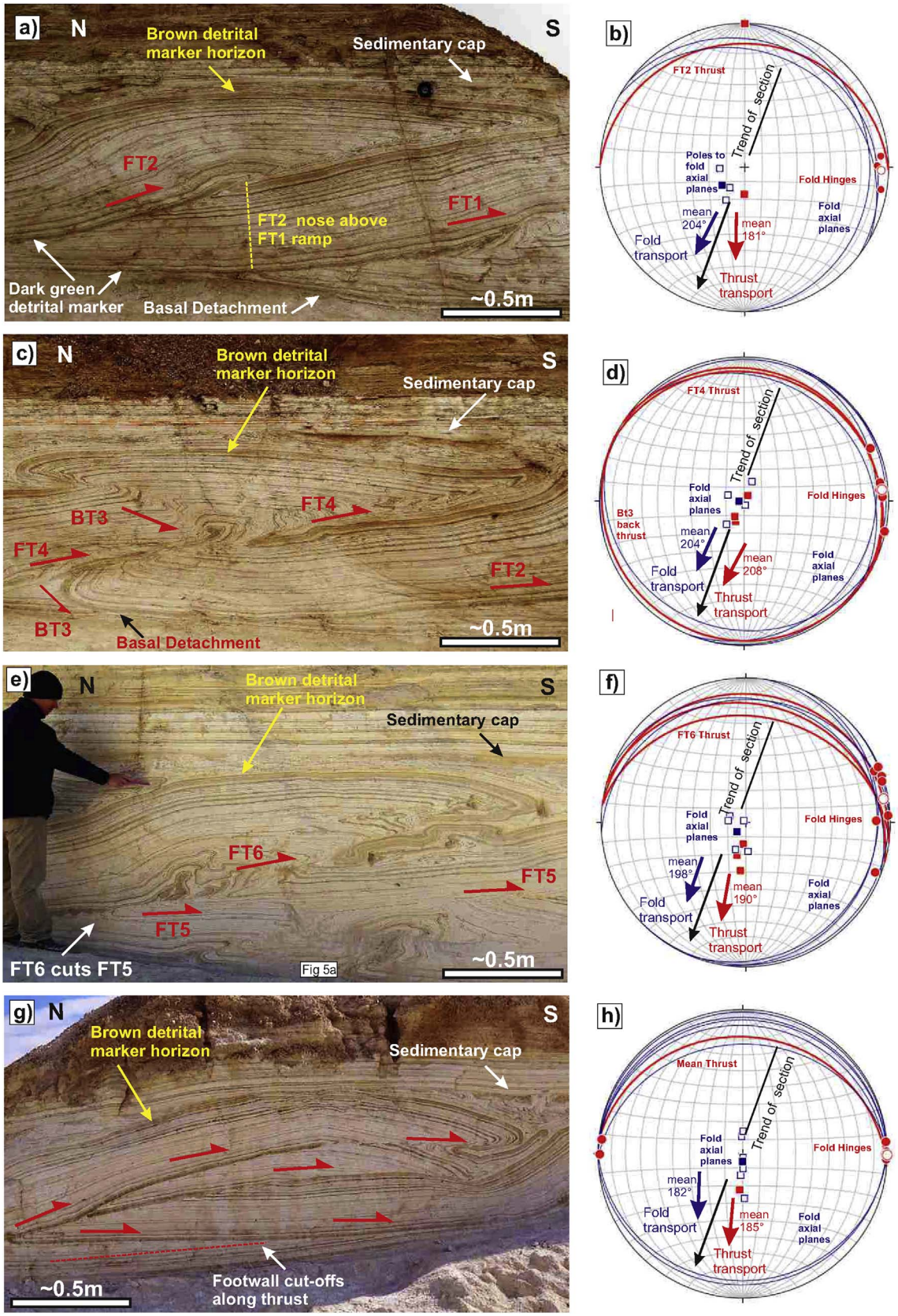

(caption on next page)

Fig. 4. Photographs (a, c, e, g) and associated stereonets of structural data (b, d, f, h) from the slumped horizon at Wadi Zin (N30°57′38″ E35°18′9″). Photograph g) has been mirrored so that south is uniformly towards the right-hand side of all photos. b) Stereonets of FT2 thrust plane (N = 1), and folds (N = 2), showing fold hinges (mean 6/091), axial planes (mean 142/16N) and thrust planes (mean strike 091°). d) Stereonets of FT4 thrust planes (N = 3), and folds (N = 5), showing fold hinges (mean 5/085), axial planes (mean 116/10N) and thrust planes (mean strike 119°). f) Stereonets of FT6 thrust planes (N = 3), and folds (N = 7), showing fold hinges (mean 4/080), axial planes (mean 137/7NE) and thrust planes (mean 100/19N). h) Stereonets of thrust planes (N = 1), and folds (N = 7), showing fold hinges (mean 0/090), axial planes (mean 093/4N) and thrust planes (mean 095/20N). Structural data on each stereonet is represented as follows: fold hinges (solid red circles), mean fold hinge (open red circle), poles to fold axial planes (open blue squares), mean pole to fold axial plane (solid blue squares), thrust planes (red great circles), and poles to thrust planes (solid red squares). Calculated slump transport directions based on fold data (blue arrows) and thrust data (red arrows) are subparallel to the trend of the outcrop section (black arrows). (For interpretation of the references to colour in this figure legend, the reader is referred to the Web version of this article.)

displacement shown by this marker across each forethrust increases in the thrust transport direction, from ~1 m displacement (FT10) at the northern end to ~ 2.5 m (FT2) at the southern end of the section (Fig. 3b and c, e, f). The maximum amount of displacement across each thrust displays a similar trend and systematically increases towards the southern end of the section. The significantly smaller displacement (~0.5 m) of the marker horizon across forethrust 6 (FT6) (Fig. 3e) is anomalous and may reflect the fact that the marker horizon is folded in the footwall of this thrust.

5. Detailed geometry and kinematics of the fold and thrust system

We now describe in detail a number of structural relationships that allow us to determine the general order of thrust development in the imbricated sequence.

5.1. Truncation of underlying folds

Upright and south-verging folds that are generated above thrust ramps and detachments are truncated by younger overlying forethrusts directed towards the south (Fig. 5a and b). This relationship suggests that folding is slightly earlier, and deformation related to thrusting has transferred to higher levels and cuts across the underlying folds. Although an increment of folding developing in advance of the thrust front is to be expected in piggyback sequences (see Butler, 1987, p.626, his Fig. 14; Morley, 1988), the repeated cutting of thrust-related folding by structurally higher thrusts supports an overstep sequence of thrusting.

5.2. Truncation of underlying forethrusts

Our observations consistently show that forethrusts directed towards the south may be cut by younger thrusts in their hangingwall (Fig. 3b and c). Within the imbricate sequence, forethrust 5 (FT5) is cut by the structurally overlying FT6 (Fig. 3b and c, 4e). Multiple systems of thrusts (T) are successively cut by younger thrusts in their hangingwall, such that T1 is cut by T2, while T2 is subsequently truncated by T3 (Fig. 5c–f). This geometry suggests that deformation and thrusting have transferred successively to higher levels, upslope towards the north, that is consistent with an overstep thrust sequence.

5.3. Truncation of underlying stratigraphy

Butler (1987, p. 627, his Fig. 17) demonstrated that overstep thrust sequences may cut up or down section in their footwall, depending on the geometry of underlying pre-existing structures. Within the study area, basal detachments cut through footwall stratigraphy that is tilted upslope (i.e. thrusts are cutting down stratigraphic section in their footwall) (Figs. 4g and 5c, d). This down-cutting in the direction of thrust transport suggests that older structures may have formed lower down, below the present surface exposure, to create a geometry described by Morley (1988, p. 541, his Fig. 2f) as reflecting out-of-sequence (or overstep) thrusting.

5.4. Loading by thrust sheets

Within areas where thrusts and associated folds overlap with one another to form imbricates, the leading 'nose' of the overlying thrust sheet is marked by a downward-directed deflection of underlying thrust sheets in their footwalls (Fig. 5 c, h). Downward deflections are associated with attenuation and 'pinching' of underlying layers, which is especially apparent when detrital marker horizons in the upper thrust sheet are in contact with equivalent markers in the underlying thrust sheet (Fig. 5c, h). In some instances, overlying thrusts remain relatively planar (e.g. T3 in Fig. 5h), while the underlying thrusts are deflected downwards (T2 in Fig. 5h), thereby suggesting that the upper thrust has depressed the underlying thrust. We therefore propose that loading from overlying thrust sheets causes downward deflections of underlying thrusts, and is consistent with an overstep thrust sequence.

5.5. Folding of thrust sheets

The order of thrust development is clearly established via cross-cutting relationships (Fig. 3b and c, 5d, section 5.2). Where the overlying and younger thrust sheets are translated above the underlying pre-existing thrusts, arching and downward facing fold noses in the younger thrusts can result (Fig. 5c, h). The downward-facing of fold noses may be further enhanced by expulsion of sediment from below thrust sheets as noted above (section 5.4). The arched thrusts and downward facing fold geometry is not a consequence of later folding, but rather the passive draping of the younger overlying thrust sheet over a pre-existing culmination created by earlier thrusts (Fig. 5c, h). The observation that the thrusts in Fig. 5c, do not meet at a common trailing point or branch line, and are intersected by the overlying thrust (T3), means that this structure is not an antiformal stack (see McClay, 1992, p.425), although it superficially resembles an antiform. This geometry is therefore consistent with overstep thrust sequences.

5.6. Extension over culminations

The passive folding and arching of thrust sheets noted above (section 5.5.) results in a series of conjugate normal faults at the crest of the culmination (Fig. 5g). These normal faults are E-W trending and are restricted to the upper portion of the uppermost thrust sheet reflecting outer-arc extension. Where normal faults continue into the overlying cap that was deposited from suspension following the failure event (Alsop and Marco, 2012b; Alsop et al., 2016), the cap displays thickening in the hangingwall of the normal fault (Fig. 5g). This observation is interpreted to represent 'growth' geometries, indicating that the normal faulting took place before and during deposition of the cap. This growth faulting, and the observation that the normal faults do not cut across the cap into the overlying sequence, demonstrates that thrusting and subsequent crestal extension was complete prior to deposition of the younger sequence. Although not considered unique to overstep thrust sequences, the outer-arc extension is thought to be a consequence of draping of the upper thrust sheet over the underlying and pre-existing culmination.

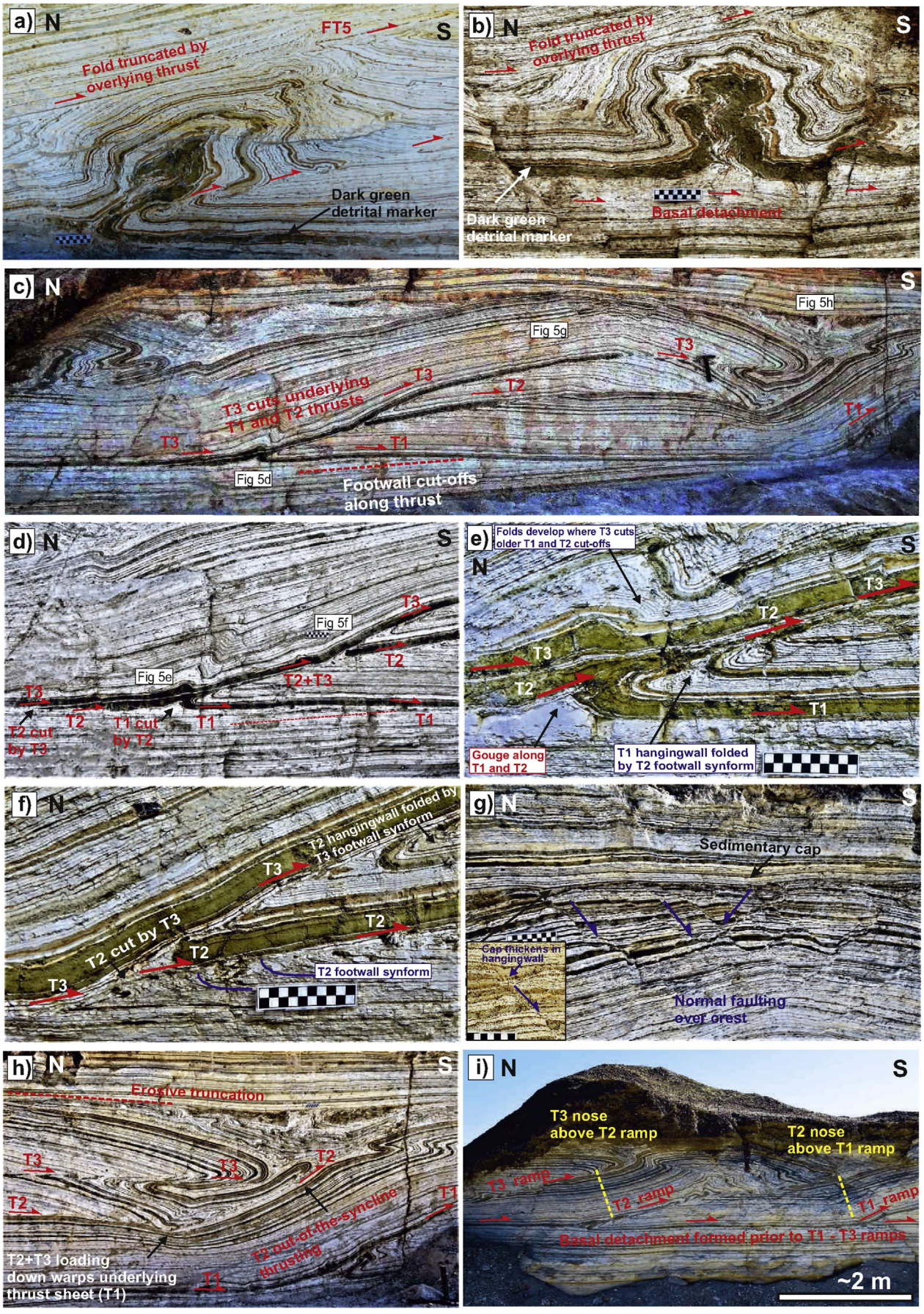

(caption on next page)

Fig. 5. Photographs of transport-parallel sections from the Zin case study (N30°57′38″ E35°18′9″). The hammer (25 cm long with 20 cm head) and chequered rule (10 cm long) act as scales. a, b) Upright folds within the dark-green detrital-rich marker horizon that are truncated by overlying thrusts. c) Overlying younger thrust (T3) cuts across older thrusts (T1, T2) in its footwall. The lowermost T1 thrust also truncates tilted stratigraphy in its footwall. d) Detail of thrust truncations shown in Fig. 5c. e, f) Details of older thrusts being folded and truncated by overlying younger thrusts (see Fig. 5d for location). g) Conjugate normal faults developed over the crest of the arched thrust sheet (T3) shown in Fig. 5c. The inset photograph highlights sedimentary thickening and 'growth' where the normal faults influence deposition of the overlying sedimentary cap. h) Deflection of older underlying thrust (T2) by overlying thrust sheet and planar T3 thrust (see Fig. 5c for position). i) Overlying thrusts (T) with noses of hangingwall anticlines positioned above ramps that branch from the underlying basal detachment. See text for further details. Photographs c, d, g, and h) are mirrored so that south is uniformly towards the righthand side of all photos. (For interpretation of the references to colour in this figure legend, the reader is referred to the Web version of this article.)

5.7. Control of underlying ramps

Where sequences of thrusts are observed, the nose of the hangingwall anticline (as defined by the competent marker horizon) within the upper thrust sheet frequently overlies the point where underlying thrusts start to steepen up and ramp from the basal detachment (Figs. 3a, 4a and 5h, i). This steepening-up of underlying thrust sheets is considered to act as a buttress and inhibit displacement along later overlying thrusts. While some of these geometries were perhaps enhanced by the effects of loading from the overlying thrusts (section 5.4), the influence exerted by underlying older thrust ramps on displacement in overlying thrusts is consistent with overstep thrust sequences.

6. Backthrusts within imbricate sequences

Backthrusts typically dip more steeply, and in an opposing direction to adjacent forethrusts in MTDs around the Dead Sea Basin (Alsop et al., 2017b) (Figs. 3b and c, 4c, 6a). Within the imbricate sequence, backthrusts (BT3, BT7, BT9) displace the marker horizon by 286 mm, 400 mm and 500 mm respectively, are convex up with dips of 35°–40° (making angles of 42° with adjacent bedding in BT3) and flatten towards their upper tips (Figs. 3b and c, 6a–e). Stratigraphy in the footwall of backthrusts may locally deflect downwards within the triangle zone, suggesting that the footwall may have been 'wedged in' during downslope-directed under-thrusting (Fig. 6b, c, d) (see Alsop et al., 2017b). These backthrusts display a number of geometric relationships to the adjacent forethrusts that permit the order of thrusting to be established, and are described below.

6.1. Truncation of backthrusts by forethrusts

Backthrust ramps represent ideal markers that may be offset by later forethrusts and therefore used to help determine the order of thrust propagation. In piggyback sequences, forethrusts may be cut by backthrusts that initiate downslope in their footwall. However, in overstep sequences, backthrust ramps are likely to be cut by forethrusts that initiate upslope in the footwall of the backthrust. Within the imbricate sequence, backthrusts (BT3, BT7) are cut and displaced by younger forethrusts in their footwall (FT4 and FT8 respectively, Fig. 3b and c, 6a, e). Cutting of backthrust ramps by younger forethrusts causes the backthrust to be folded into hangingwall anticlines and footwall synclines linked to the younger thrust (Fig. 6a–e). The backthrust can then no longer operate as it becomes 'locked-up' and inactive, thereby producing relatively small displacements on the backthrusts (< 400 mm in BT3 and BT7). The hangingwall sequence above FT4 dips gently towards the south in the direction of thrusting, suggesting that the younger forethrust has not fully compensated and rotated the sequence that would have dipped in the direction of thrusting above the steeper BT3 (Fig. 6a).

6.2. Truncation of forethrusts by backthrusts

Within the imbricated sequence, backthrust BT9 at the northern end of the section cuts FT8 (Fig. 3b and c, 6d). While the backthrust (BT9) ramps off the basal detachment, FT8 does not cut down onto the basal detachment, but forms a flat ~10 cm above the imbricated lower detrital layer (Fig. 6c, d, e). This difference in the levels of the backthrust and forethrust flats permits the younger backthrust to cut the forethrust in its hangingwall (Fig. 6d). In addition, downslope-verging folds developed in the hangingwall of the forethrust flat (FT8) may be subsequently tilted downslope, to become downward-facing, as they are translated along the BT9 ramp (Fig. 6d). This backthrust (BT9) dips at 40° and causes stratigraphy in its footwall to be deflected downwards as the upslope wedge is 'driven-in' (see Alsop et al., 2017b). In summary, FT8 cuts and displaces BT7, but is itself cut by BT9, providing a clear sequence of thrusting that gets progressively younger towards the north, in the upslope direction, and therefore collectively defines an overstep thrust sequence.

7. Folding of detachments and 'short-cut' thrusts

7.1. Basal detachment

The basal detachment is universally developed immediately below a 5 cm thick dark green detrital-rich layer (Figs. 3a, 4a and 6a). This discontinuity locally cuts obliquely across beds in the footwall that are tilted gently upslope (Figs. 5c and 7a, b). Some thrust ramps branch directly from the basal detachment, and define overstep sequences with underlying thrusts and folds truncated and offset by overlying (younger) thrusts (Fig. 7a, c). This behaviour may result in fold hinges within the dark green detrital layer becoming progressively 'detached' and isolated by younger thrusts cutting across them (Fig. 7c). In other instances, thrust ramps initiate in the hangingwall of the basal detachment, and fail to propagate downwards across the green detrital marker to join the underlying detachment (Fig. 7d).

The basal detachment itself is generally < 1 cm thick, although it locally forms a zone up to ~5 cm thick marked by disrupted beds (Fig. 7e) with extensional shears (Fig. 7f) and several individual detachments (Fig. 7g). The base of the detachment zone is generally a sharp planar discontinuity, while individual strands of the detachment system are locally observed to cut into the dark green marker layer (Fig. 7h). The top of the detachment zone is marked by a gouge layer directly beneath the dark green detrital bed (Fig. 7g and h). The gouge is generally light grey to buff coloured, up to 30 mm thick, and is similar to gouge horizons formed along bedding-parallel slip surfaces observed elsewhere in the Lisan Formation (Weinberger et al., 2016) (Fig. 7b, d–h). Locally, the underlying sediment and gouge within the basal detachment zone penetrate upwards as small 'fingers' into the overlying dark green detrital marker (Fig. 7i and j). We speculate that this dark green layer significantly controlled the depth to basal detachment at ~0.8 m, with potential increases in pore fluid pressure directly below this marker causing the injection of sediment fingers.

7.2. Fault gouge and thrust ramps

While thrust displacement along bedding-parallel flats and basal detachments may be difficult to determine due to the lack of suitable offset markers, the position of thrust ramps is clearly shown by displacement of bedding. In addition, a locally developed fault gouge up to 20 mm thick and extending for tens of cm is formed along the thrust ramps (Figs. 7g–j, 8a-d). The gouge comprises disaggregated grains and fragments of white aragonite and dark detrital-rich sediment that are mixed together to form the light grey-buff gouge (Fig. 8a, c). The gouge is sometimes bordered by 10 mm thick brecciated zones, where dark

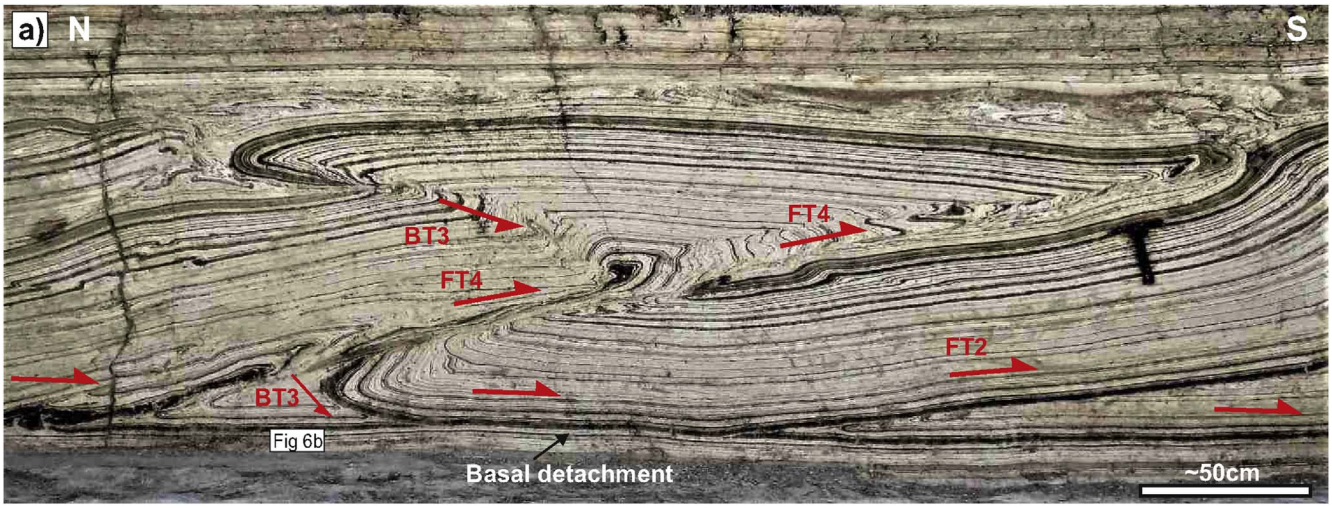

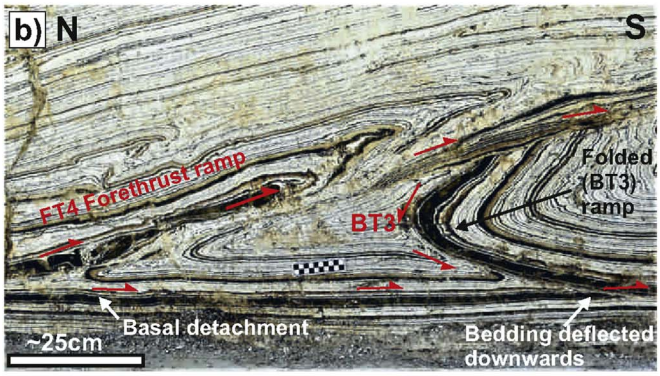

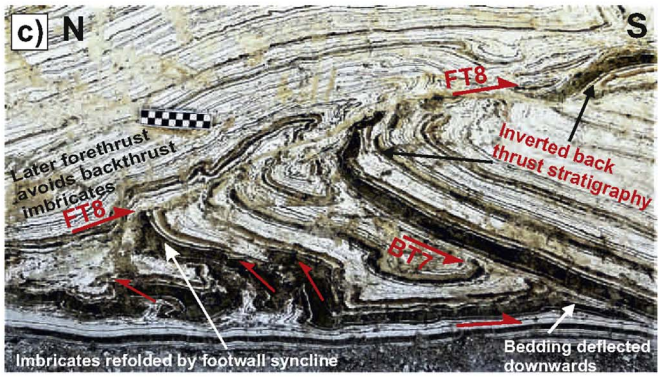

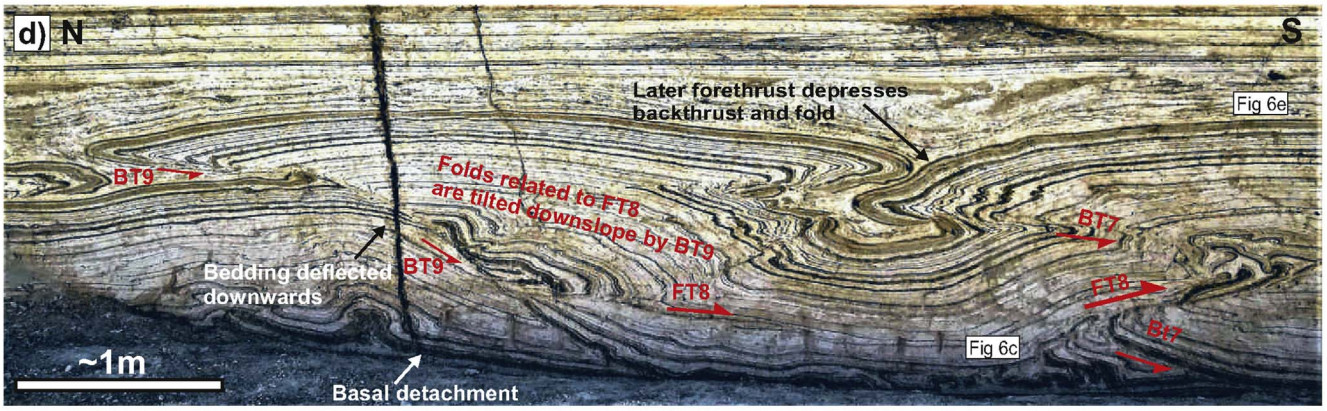

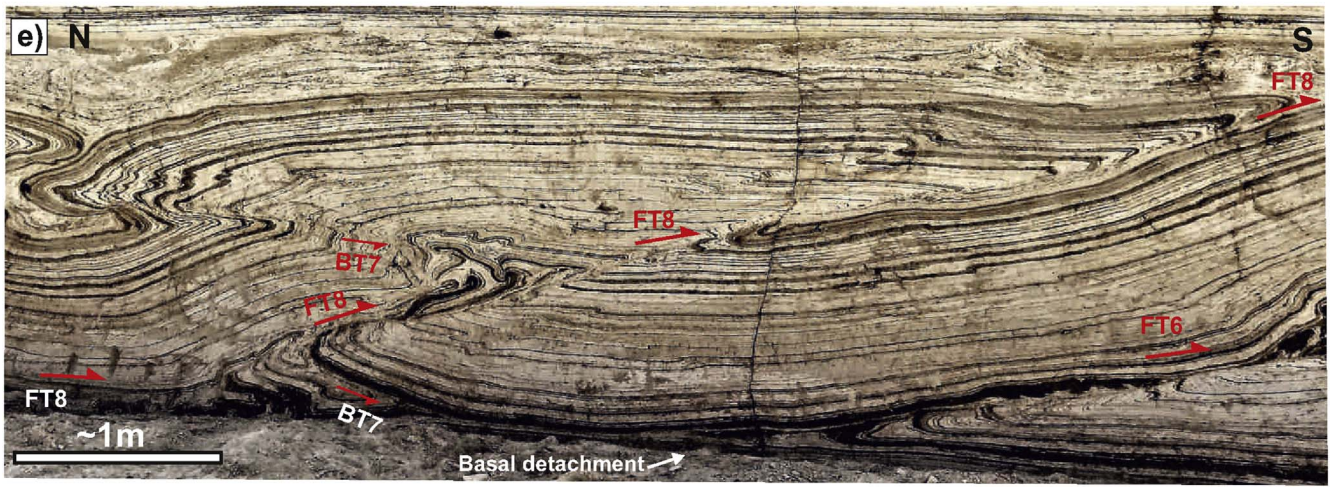

(caption on next page)

Fig. 6. Photographs from the transport-parallel trench at the Zin case study (N30°57′38″ E35°18′9″). The chequered rule (10 cm long) and 25 cm long hammer act as a scale. Refer to Fig. 3b and c for details of location of forethrusts and backthrusts. a) Backthrust 3 (BT3) is cut and displaced by a younger forethrust (FT4) that developed upslope in its footwall. The 'pop-up block' in the hangingwalls of BT3 and FT4 is tilted gently downslope (to the south). b) Details of BT3 and FT4 branching from the same basal detachment, with BT3 being folded into a footwall syncline along FT4. Position shown in Fig. 6a. c) Details of the imbrication of dark-green detrital rich marker horizon in the footwall of BT7. These imbricates are cut across by the younger FT8. Position shown in Fig. 6d. d) Details of BT9 that truncates FT8 and its associated south-verging folds. Folds are interpreted to have been tilted by BT9 to become downward-facing towards the south. The stratigraphy forming the footwall to BT9 is marked by pronounced downward deflection towards the south. e) Backthrust 7 (BT7) is truncated and folded by forethrust 8 (FT8) that develops upslope (towards the north). See text for further details. (For interpretation of the references to colour in this figure legend, the reader is referred to the Web version of this article.)

detrital-rich horizons are broken into mm-scale fragments (Fig. 8a). In some cases, the breccia zone is bordered on both sides by extremely fine-grained gouge that truncates bedding laminae above and below the breccia (Fig. 8b). The thickness of the breccia and gouge horizons does not appear to correlate with the displacement magnitudes across the thrusts, with gouge perhaps best developed where thrusts cut directly across aragonite- and detrital-rich layers in their footwall and hangingwall. Anisotropy of magnetic susceptibility (AMS) studies (Weinberger et al., 2017) within the gouge developed along FT4 (Fig. 6a and b) reveal a predominantly oblate fabric and thrust transport towards the south. Taken with the development of gouge-flanking breccia, our observations suggest that once breccia and gouge horizons developed, they were relatively weak and focussed continued slip, rather than becoming wider zones of deformation (see Weinberger et al., 2016).

7.3. Detachments and 'short-cut' thrusts

Detailed examination of gouge reveals that it may be locally thrust and displaced (Fig. 8e). In addition, gouge may form along basal detachments that are developed below detachment folds (Fig. 8f). Parts of the gouge are displaced and imbricated within the core of such folds, while the main horizon of gouge is present along the basal detachment (Fig. 8f). This relationship suggests that while earlier-formed gouge is imbricated, new gouge forms along the basal detachment during continued translation. Similar patterns of multiple generations of gouge are observed around footwall synclines positioned immediately beneath where thrusts ramp from the basal detachment (Fig. 8g–j). Gouge formed along the basal detachment is locally imbricated and thrust within the footwall syncline (Fig. 8h, i, j), while the underlying basal detachment is also marked by gouge beneath the imbricated zone. We interpret this geometry to reflect imbrication and folding of early formed gouge along the basal detachment, with new gouge then forming along a 'short-cut' fault that defines a new basal detachment below the syncline during continued movement (section 9.4.1.).

8. Displacement –distance plots

Displacement-distance analysis involves measuring the distance along the hangingwall of a thrust from a fixed reference point ('R' near the fault tip) to a marker horizon, and comparing this distance with the displacement of that marker across the thrust (Muraoka and Kamata, 1983; Williams and Chapman, 1983; Chapman and Williams, 1984) (Fig. 9a). The process is then repeated for different marker beds along the length of the fault to create a displacement-distance (D-D) plot for that fault. In general, steeper gradients on D-D plots represent slower propagation of the thrust tip relative to slip accrual in weaker units, while gentle gradients on D-D plots represent more rapid propagation of the thrust tip relative to slip accrual in stronger or more competent units (e.g. Williams and Chapman, 1983; Ferrill et al., 2016). As displacement on faults is typically assumed to be time-dependent, then older portions of faults are assumed to accumulate the greatest displacement (e.g. Ellis and Dunlap, 1988; Hedlund, 1997; Kim and Sanderson, 2005). The point of maximum displacement on a D-D plot is therefore typically interpreted to represent the site of nucleation of a fault (e.g. Ellis and Dunlap, 1988; Peacock and Sanderson, 1996; Hedlund, 1997; Ferrill et al., 2016).

In the Zin case study, displacement-distance (D-D) plots across thrust ramps, which root downwards onto the basal detachment of the system, show the greatest displacement at the lowermost part of the ramp, or further up the ramp itself (Fig. 9a–j). Unlike forethrusts developed in piggyback sequences elsewhere in the Lisan Formation (Alsop et al., 2017a), the forethrusts analysed in this study do not display simple linear displacement-distance relationships (Fig. 9a–j). In some cases, the greatest displacement is developed further up the ramp, to create 'hook shaped' D-D profiles (Fig. 9a–f). In other cases, the D-D profiles display distinct steps and jumps which correlate with where the thrusts cuts detrital markers (Fig. 9e, f, i, j), or pre-existing thrusts in their footwall (e.g. Fig. 9g and h). Displacement-distance data from a thrust ramp developed within the hinge of a hangingwall anticline above FT6 (labelled FTa in Fig. 9g and h) reveals marked displacement gradients towards both its lower and more especially upper tips, and demonstrates that pronounced displacement gradients are an important feature of thrusts cutting unlithified sediments. Overall, the steepest displacement gradients consistently developed towards the upper fault tip (Fig. 9a–j). These relationships collectively suggest that thrust ramps do not always propagate upwards from the underlying basal detachment, which must have already been present in an overstep sequence, but initiated in the hangingwall of the detachment (e.g. Fig. 7d). Individual thrust ramps that display a number of displacement maxima are inferred to be thrusts that possibly formed via amalgamation of several smaller fault strands (Fig. 9g–j) (Alsop et al., 2017a).

9. Discussion

Our structural analysis demonstrates that a south-directed fold and thrust imbricated sequence formed within the case study (Figs. 3 and 4). This south-verging MTD is directed away from the Dead Sea, and clearly does not form part of a radial pattern of slumping developed further north, which verges towards the depocentre of the basin (Alsop and Marco, 2012a), This apparently anomalous situation can be explained by tilting of large-scale fault blocks associated with the NW-SE trending Amazyahu Fault, which was active during deposition of the Lisan Formation and is developed immediately to the NE of the study area (Fig. 1b, d) (Smit et al., 2008; Weinberger et al., 2017). Gentle tectonic tilting of fault blocks by just a few degrees across this NE-dipping listric transverse fault system (Smit et al., 2008) would be sufficient to alter directions of slope failure and gravity-driven MTD emplacement during deposition of the Lisan Formation (Alsop and Marco, 2012a, 2013).

9.1. What criteria can be used to distinguish different thrust sequences?

9.1.1. Cross-cutting relationships

The most straightforward criteria to establish order of thrust development are cross-cutting relationships between thrusts themselves. Butler (1987, p. 619) stated that overstep geometries are marked by earlier structures being truncated in the footwall of a later fault. Thus, in our study, thrusts are subsequently truncated by overlying thrusts and are therefore indicative of an overstep sequence (e.g. Figs. 4e and 5c, d, 10). In addition, folds that detach on underlying thrusts are also cut by overlying thrusts supporting an overstep sequence (e.g. Fig. 5a and b, 7a, 10). Similar observations of folds being truncated by overlying thrusts have also been reported from outcrop studies of other

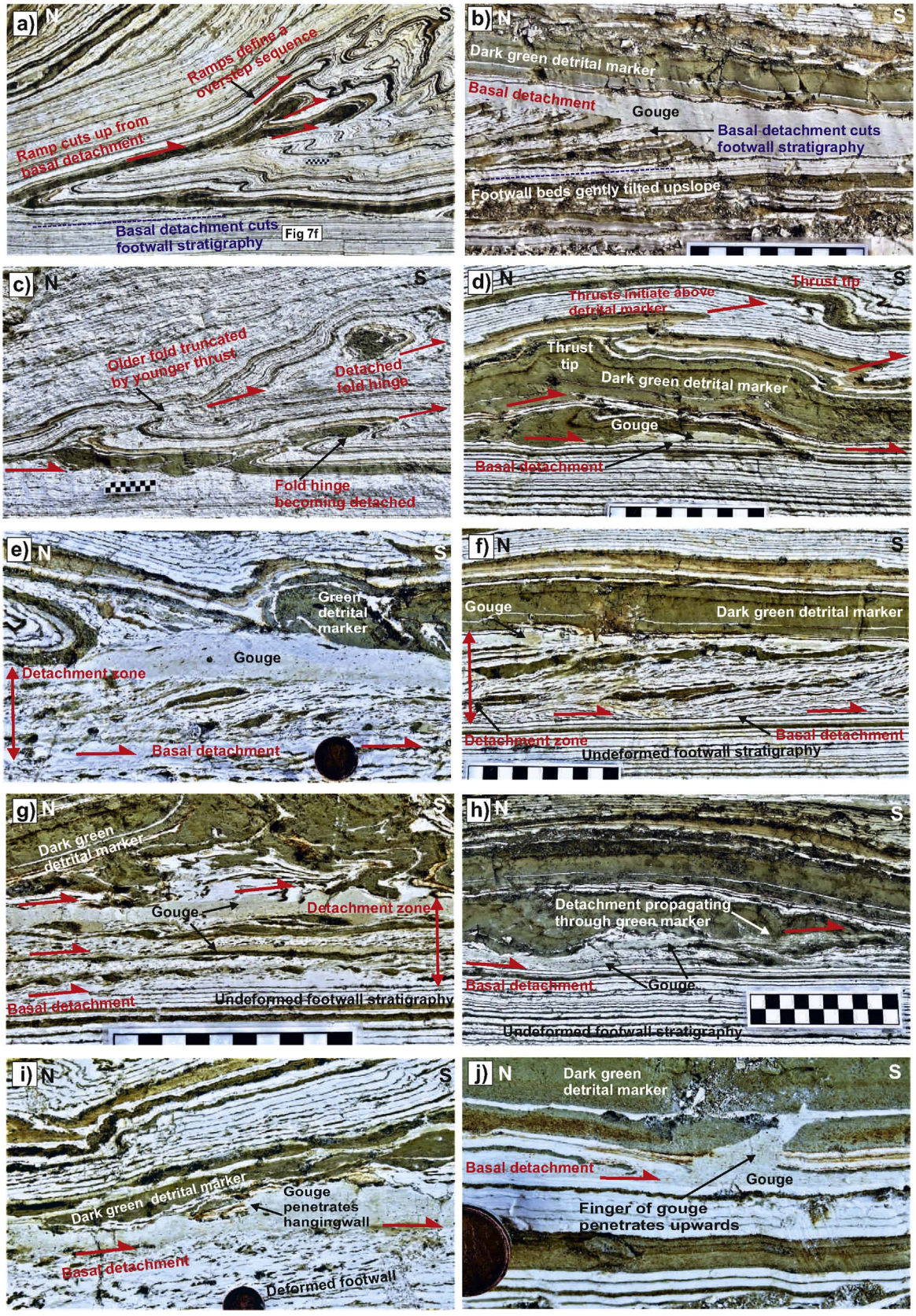

(caption on next page)

Fig. 7. Photographs of the basal detachment and directly overlying dark green detrital rich marker bed. a, b) Basal detachment cuts across footwall stratigraphy that is gently-dipping upslope. In a) fold hinges are cut across by overlying thrusts in an overstep sequence. c) Thrusts ramping up from the basal detachment that cut existing folds forming detached fold hinges within the dark green marker layer. d) Thrusts developed in the hangingwall of the basal detachment fail to propagate downwards through the dark green marker layer. e, f) Basal detachment marked by an intensely deformed ~5 cm thick zone beneath the dark green marker. The base of the detachment zone is a planar discontinuity, while the top displays fault gouge. g) Basal detachment zone marked by several individual detachment strands that in h) are locally interpreted to propagate through the detrital marker. i) The top of the detachment zone is marked by fault gouge that locally truncates the overlying hangingwall stratigraphy. j) Basal detachment beneath a backthrust (BT3) that displays a 'finger' and injection of gouge and sediment up into the overlying dark green detrital marker. 10 cm long chequered rule and 15 mm diameter coin for scale. (For interpretation of the references to colour in this figure legend, the reader is referred to the Web version of this article.)

MTDs (e.g. Strachan, 2002, p.32, her Fig. 7a).

9.1.2. Loading and deflection of underlying thrusts

The effects of loading by overlying thrust sheets are most pronounced where competent marker horizons impinge directly on one another, and where the overlying thrust sheet comprises a recumbent fold nose (e.g. Figs. 3a and 5c, h). Loading may locally depress underlying thrusts to create upright synforms (e.g. T2 in Fig. 5h), while the overriding thrust remains relatively planar (e.g. T3 in Fig. 5h). This suggests that T3 generated the loading, and while there may be some local 'out-of-the syncline' movement along T2, which caused displacement of the marker horizon, T2 effectively became 'locked' due to its folded geometry (Fig. 10). Overlying thrusts loading and deforming underlying thrusts is suggestive of an overstep thrust sequence (e.g. Fig. 5h).

9.1.3. Structural inheritance from underlying thrusts

Structural inheritance whereby the extent and geometry of an overlying thrust is controlled by the geometry of the underlying structure may also be used to determine the sequence of thrust development (e.g. Fig. 5i). Following Dahlstrom (1970, p.352), Boyer and Elliot (1982, p.1207) note that "a higher horse is folded over a lower one proving forward development". However, in the case study, where higher thrust sheets (horses) are folded over lower ones, then the higher sheet clearly truncates the underlying thrust (Fig. 5c and d). Thus, although the overall geometry of Fig. 5c broadly resembles an 'antiformal stack' (e.g. Butler, 1987, p. 621), detailed relationships and the lack of a common trailing branch line (e.g. McClay, 1992, p.425) demonstrate an overstep rather than a piggyback sequence.

In summary, these three primary strands of evidence collectively demonstrate a predominant overstep sequence of thrusting (Fig. 10). Although overstep thrusting has long been suggested to occur during slumping of sediments (e.g. Farrell, 1984), this detailed study of such a sequence within a gravity-driven fold and thrust belt is the first to document the sequencing.

9.2. What are the cross-cutting relationships between forethrusts and backthrusts?

In gravity-driven MTDs, fold and thrust systems will translate and verge down the regional slope (Fig. 10). In downslope-propagating piggyback thrust sequences (Fig. 1a), it is more likely that younger backthrusts developed in the footwalls of forethrusts will cut the forethrusts (Fig. 11a), whereas if backthrusts develop first they may be translated up the ramp of the later forethrust (Fig. 11b). No such relationships relating to downslope-propagating thrust systems have been observed in the case study. Conversely, in upslope propagating overstep sequences (Fig. 1b), oppositely dipping backthrusts are more prone to being cut by younger forethrusts developed further upslope (Fig. 11c), while older forethrusts may be truncated and carried in the hangingwall of younger backthrusts (Fig. 11d). The relationships observed in the case study where older backthrusts are cut by younger forethrusts developed upslope (e.g. BT3, BT7 in Fig. 6a, e relates to Fig. 11c), or older forethrusts are cut by younger backthrusts upslope (e.g. BT9 in Fig. 6d relates to Fig. 11d) are entirely consistent with an overstep sequence of thrust development.

9.3. Why do overstep thrust sequences develop?

When discussing orogenic thrust belts, Butler (1982, p. 241) noted that "overstep thrust sequences are rarely recognised and, hence, the geometry of such thrust splays is not well described". Although local examples of overstep sequences within orogenic belts are documented (e.g. Butler and Coward, 1984; Coward, 1985; Butler, 1987), a foreland-propagating or piggyback system of thrusting is generally applied to thrust belts. Morley (1988, p.540) suggested that any individual 'random' thrust, or sequence of thrusts that follows a break-back (overstep) sequence should be termed out-of-sequence and provided some general examples. In addition, Butler and McCaffrey (2004, p.916) described a clear km-scale example of an individual break-back or overstep sequence in the Alps of SE France. In this example, folding of thrust ramps lead to new short-cut thrusts forming in the hangingwall that truncated the underlying thrust ramp.

Within MTDs, Farrell (1984, p.735) noted that if movement of the slumped mass ceases first at the downslope toe, perhaps due to a reduction in slope gradient, then continued downslope movement of the portions of the slump further upslope will lead to a late-stage contractional strain wave propagating back up the slumped mass (see also Strachan and Alsop, 2006; Alsop and Marco, 2011, 2014). This behaviour will generate downslope-verging folds and thrusts that form at a relatively late-stage and get progressively younger back up the slope in an overall overstep sequence (Fig. 1b). A number of studies do indeed invoke an upslope-propagating contractional strain wave to create late-stage thrusts such as observed in Carboniferous-aged slumps of western Ireland (Martinsen and Bakken, 1990; Strachan and Alsop, 2006) or Miocene-aged slumps of New Zealand (Strachan, 2008), although details of the exact timing relationships between thrusts are lacking in these cases. Thus, despite such overstep thrust sequences having long been assumed to operate during cessation of downslope movement within sediments, we have not found existing detailed descriptions of such thrust sequences developed in gravity-driven fold and thrust belts.

Within the Zin case study, we have demonstrated that slump transport is directed towards the south, resulting in an overstep thrust sequence where structures get younger up the depositional slope towards the north (see section 10.1.) (Fig. 3b and c). However, evidence is lacking for an earlier deformation with significant structures that predate the thrusts, and the fold and thrust imbricates cannot therefore be regarded as 'late stage' features. We propose that similar overstep thrust sequences will be created if movement towards the toe of the MTD simply reduces velocity compared to more rapid translation of the slumped mass further upslope. We suggest that in this case, the overstep sequence is not linked to cessation of movement but was created during variable rates of downslope flow during actual translation of the MTD. Furthermore, if second-order cells of variable flow were developed during translation (Alsop and Marco, 2014), then local sequences of overstep thrusting could form throughout the gravity-driven fold and thrust belt.

9.4. Can some thrusts move synchronously?

Despite the common expectation that piggyback thrusting occurs, it has long been recognised that "it is unrealistic to expect older thrusts to be deactivated as movement is transferred to younger thrusts" (Boyer, 1992, p.386). Indeed, a number of authors including Morley (1988),

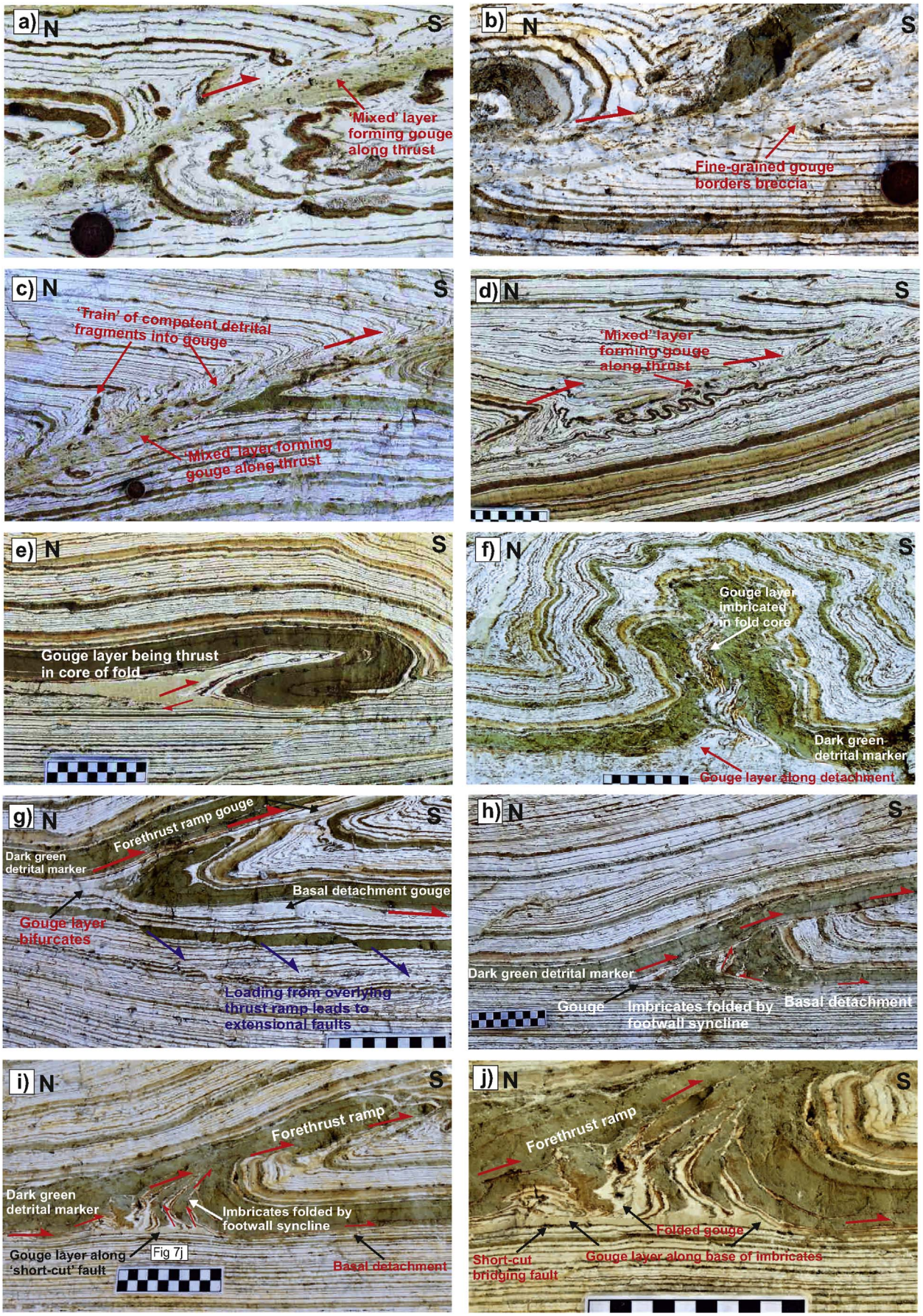

(caption on next page)

Fig. 8. Photographs (a, b, c, d) of fault gouge developed along thrust imbricate ramps from the Zin cutting. The light-grey or buff colour of the gouge is created by mixing of aragonite- and detrital-rich laminae that are truncated by the thrust. e) Gouge horizon cut by a small thrust associated with an overlying fold pair picked out by the dark-green detrital rich marker horizon. f) Upright detachment fold that deforms the dark-green detrital rich marker horizon. The gouge horizon is folded and imbricated within the fold core, but also is developed along the underlying basal detachment to the fold. Photograph f) has been mirrored so that south is uniformly towards the righthand side of all photos. g) Bifurcation and folding of gouge horizon along a fore thrust ramp and basal detachment below the dark-green marker horizon. h) Imbricates marked by gouge horizons folded into a footwall syncline defined by the dark green marker horizon. i, j) Imbricates marked by gouge horizons folded into a footwall syncline. New gouge is developed along a 'short-cut' fault that forms a new basal detachment along the base of the imbricates. The chequered rule (10 cm long) and 15 mm diameter coin act as scales. (For interpretation of the references to colour in this figure legend, the reader is referred to the Web version of this article.)

Boyer (1992, p. 377) and Butler (2004, p.2) suggest that thrusts may have been active synchronously in many orogenic belts. Totake et al. (2017) utilizing seismic reflection data across an offshore fold and thrust belt that may be driven by a combination of both collisional plate tectonics and gravitational failure of the slope emphasise that "fold structures and their underlying thrusts were not active in a strict sequence" and that "structures were active in parallel" (i.e. synchronous). Synchronous development of thrust systems has also been proposed by Cruciani et al. (2017) within gravity-driven fold and thrust belts within MTDs. Based on modelling, Liu and Dixon (1995, p.885) also noted that "early formed thrusts continue to accumulate displacement even while new ones are nucleating". We therefore discuss some of the features associated with synchronous thrusting in MTDs from the Zin case study (Fig. 1c).

9.4.1. Folding of earlier detachments

In piggyback systems, earlier thrust ramps are abandoned and may be passively carried in the hangingwall of younger underlying ramps (e.g. Butler, 1987, p. 620) (Fig. 1a). The entire underlying basal detachment or floor thrust is generally considered to be active throughout this process (Fig. 1a). Conversely, in overstep sequences, the foreland, or downslope, portions of the underlying basal detachment are progressively abandoned as the locus of displacement propagates back towards the hinterland, or upslope (Fig. 1b). Upslope propagation of downslope-verging overstep sequences may result in basal detachments being folded by footwall synclines as they become sequentially abandoned (Fig. 10). Where a basal detachment is tightly folded then it can no longer be active. Within our study, the basal detachment may be folded around the footwall syncline of forethrusts, leading to local imbrication (Fig. 8h, i, j). In other cases, bridging 'short-cut' faults marked by gouge layers run along the base of the footwall syncline, indicating that the basal detachment was still active and did not lock-up (Fig. 8f–j).

We suggest that downslope thrusts and basal detachment may have continued to move, but not as rapidly as upslope thrusts. This behaviour would produce short-cut faults and gouge layers developed below folded detachments as downslope movement continued during synchronous thrusting (Fig. 10).

9.4.2. Systematic increase in displacement across imbricates

If early-formed thrusts remain active as newer thrusts develop, and assuming thrust displacement rates have remained fairly constant, then older thrusts should accrue larger displacements (Boyer, 1992, p.384) (Fig. 1c). Seismic sections across the Orange Basin offshore Namibia reveal "Displacement on individual faults increases progressively from the deformation front to the inner part of the contractional domain" (de Vera et al., 2010, p.229). Within this piggyback system of thrusting (de Vera et al., 2010), such a systematic increase upslope towards the presumed older thrusts suggests that a component of synchronous thrusting may also have operated. In the case of broadly overstep sequences associated with a component of synchronous thrusting, greater displacements should therefore be observed in the downslope portion of the gravity-driven fold and thrust belt adjacent to the toe (Fig. 1c). Indeed, many interpretations of slumps and MTDs suggest increasing deformation towards the toe (e.g. Cruciani et al., 2017). The section through the imbricated overstep sequence clearly displays a systematic increase in displacement in the direction of thrust transport and vergence (Fig. 3b–f). Forethrust 6 (FT6) forms the single exception to this general trend, which may relate to FT6 cutting through earlier upright folds of the competent detrital marker layer causing the thrust to take a slightly steeper trajectory, before it can create a bedding-parallel flat above the marker (Fig. 4e). Where FT6 has cut through this competent marker, a distinct step in the displacement-distance plot is observed (Fig. 9g, f). In addition, FT6 truncates earlier thrusts (FT5) in its footwall (Fig. 4e) (section 4.1.), while FT6 is itself cut across by a younger upslope backthrust (BT7) that may have truncated and 'locked-up' the forethrust before it had opportunity for displacement to grow further (Fig. 3b–f).

In summary, pre-existing or subsequently formed structures may influence displacement on imbricates, although the overall progressive increase in displacement downslope towards the toe indicates synchronous thrusting of an overstep sequence.

9.4.3. Displacement on backthrusts

Backthrusts typically have much smaller displacements than adjacent forethrusts with < 500 mm displacement of the marker horizon on BT3, BT7 and BT9 (e.g. Fig. 3b–c) and is partially a consequence of backthrusts being steeper than forethrusts, so that they are less efficient at accommodating horizontal shortening. However, backthrusts may not have a large component of synchronous thrusting displacement as they are folded and truncated by later overlying forethrusts in an overstep sequence. This truncation and dislocation effectively 'locks-up' the backthrusts causing them to become abandoned. Backthrusts that are not cut across by forethrusts may have slightly larger displacements (e.g. BT9 in Fig. 3b and c). In general, synchronous thrusting is hindered and reduced by thrusts that cut across one another thereby leading to abandonment of the displaced thrust plane.

9.5. How do displacement-distance plots relate to overstep thrust sequences?

9.5.1. Displacement on thrust ramps

As noted previously (Alsop et al., 2017a), displacement-distance (D-D) patterns are much more variable along thrust ramps cutting unlithified sediments compared to those plots from thrusts in lithified sequences. Analysis of D-D plots from seismic sections across large-scale MTDs in offshore setting suggests that the greatest displacement may occur near the basal detachment/shear zone, and that this displacement progressively diminishes up the thrust ramp (Frey-Martinez et al., 2006, p.595). However, in some instances within our study, displacement does not reduce significantly towards the apparent fault tip leaving the displacement profile 'detached' from the tip (e.g. Fig. 9g–j). Such profiles are most obvious where thrusts have a ramp geometry through tilted stratigraphy in the underlying thrust sheet (Fig. 9e and f, 9i, j). This relationship suggests that some faults may follow a bedding-parallel 'flat' trajectory above the upper marker, with the actual fault tip potentially located further downslope. However, marked displacement gradients towards both upper and lower thrust tips in other cases are constrained by adjacent stratigraphy, thereby demonstrating that such gradients are genuine and not an artefact of measurement error (Fig. 9g and h) (see also Alsop et al., 2017a, b).

Similar pronounced gradients in fault displacement have been identified by Butler and McCaffrey (2004) who described km-scale thrusts that locally display break-back (overstep) sequences cutting weakly lithified turbidites in the Alps. Butler and McCaffrey (2004,

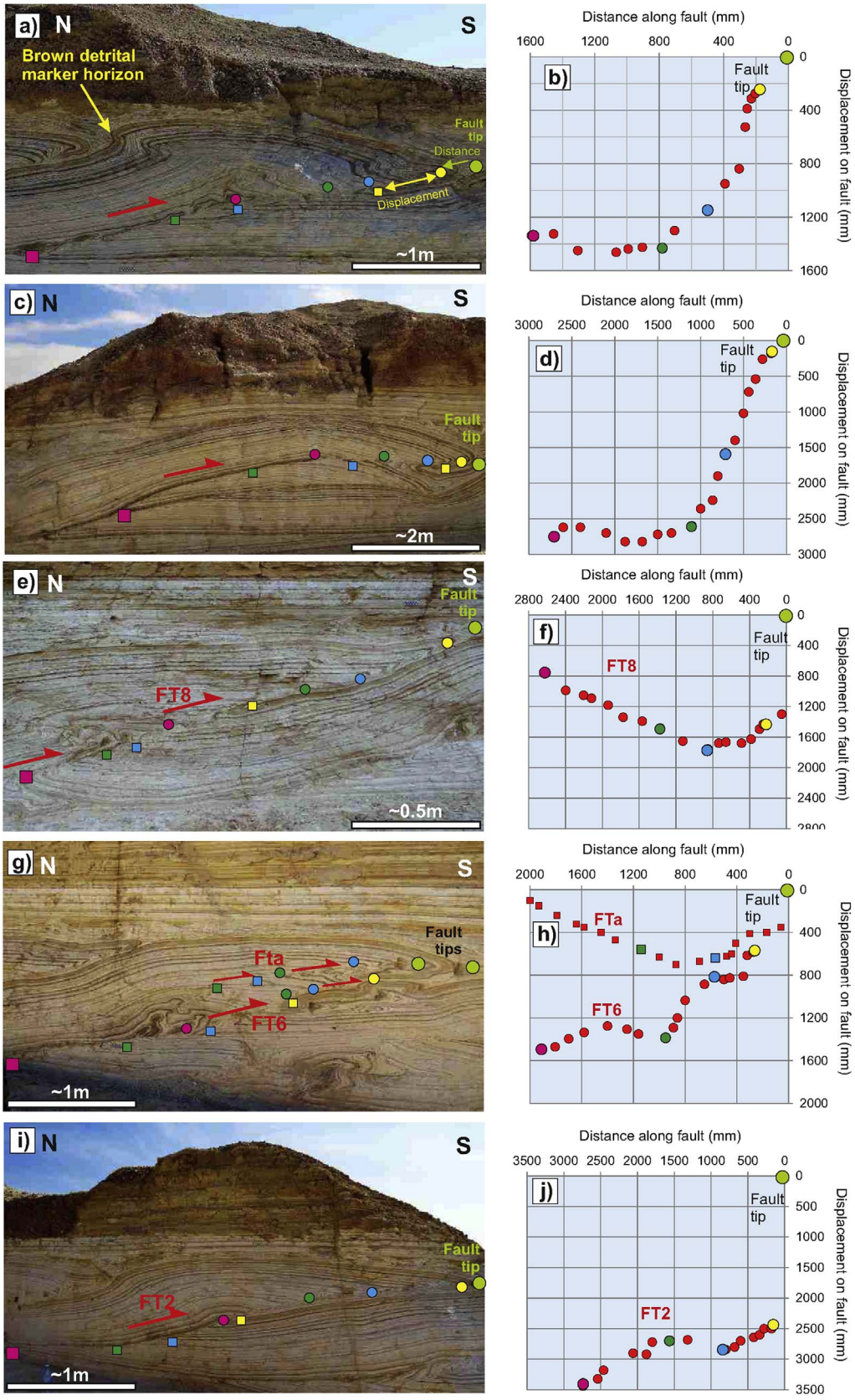

Fig. 9. Photographs (a, c, e, g, i) and associated displacement-distance plots (b, d, f, h, j) across thrusts in the Zin case study. Photograph c) has been mirrored so that south is uniformly towards the right-hand side on all photographs. Displaced marker horizons are highlighted on photographs by coloured squares (footwall) and circles (hangingwall), with displacement dying out at the fault tip (light green circle). Equivalent horizons on displacement-distance plots are shown by matching coloured circles, while red circles correspond to intervening displaced beds. Measurements of distance from the fault tip and displacement of the yellow markers are illustrated on a). A 10 cm thick detrital-rich competent horizon is highlighted by a yellow marker in each case (as also shown in Fig. 3c). Note that fore thrust numbering (FT2, FT6, FT8) is used to denote order of ramp development as shown in Fig. 3b and c. In g, h), displacement-distance across a smaller thrust (FTa) that displays pronounced displacement gradients towards the fault tips is also shown. (For interpretation of the references to colour in this figure legend, the reader is referred to the Web version of this article.)

p.916) measured steep gradients in along-strike shortening that is more than an order of magnitude greater than is expected using Elliot (1976) 'bow and arrow' rule of 10% variation for shallow thrust system in lithified rocks. Seismic studies of a 350 km long and 70 km wide offshore deepwater fold and thrust belt by Totake et al. (2017), who measured thrust heave, thereby avoiding uncertain depth conversion on seismic, found "high heave gradients of the master thrusts" that is consistent with restricted fault-tip propagation (Totake et al., 2017). It would

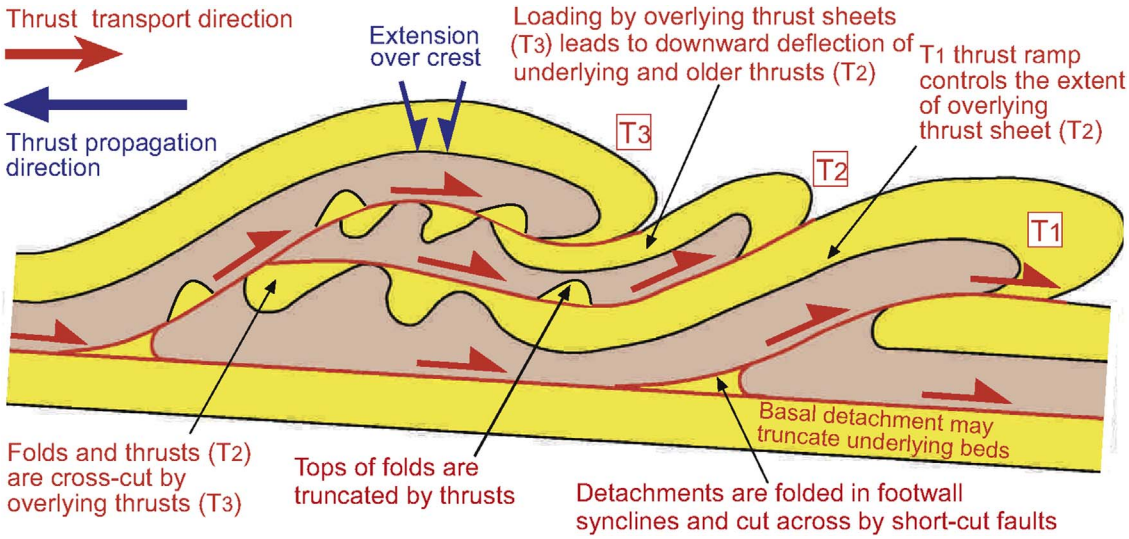

Fig. 10. Summary cartoon highlighting some of the main features developed during an overstep thrust sequence that continues to undergo synchronous thrusting. Thrusts (T) are numbered according to the order of development (T1, T2 etc.) while the directions of thrust transport (large red arrow) and overall thrust propagation (blue arrow) are also shown. Refer to text for further details. (For interpretation of the references to colour in this figure legend, the reader is referred to the Web version of this article.)

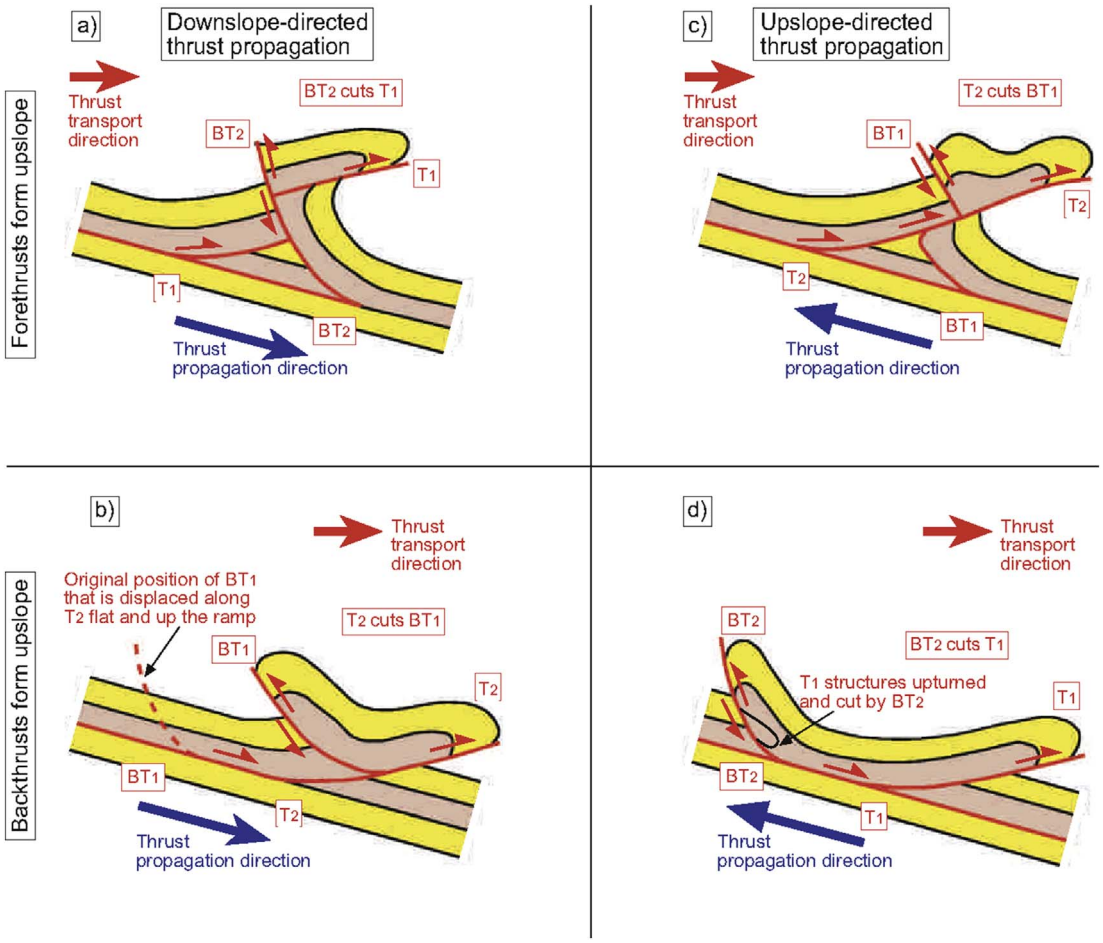

Fig. 11. Summary cartoons illustrating the four possible end-member scenarios of forethrust (T) and backthrust (BT) interaction. The thrusts are numbered according to their relative timing (T1, BT2 etc.) where the resulting structural geometries depend on relative timing and position of each thrust. Directions of thrust transport (large red arrows) and overall thrust propagation (blue arrows) down (a, b) or up (c, d) the regional slope are also shown. (For interpretation of the references to colour in this figure legend, the reader is referred to the Web version of this article.)

appear therefore that pronounced displacement-distance gradients are not restricted to m-scale structures within fold and thrust systems of our study, but also ocurred along km-scale thrusts cutting weakly lithified sediments and are therefore scale independent.

Models of thrust ramp propagation by linking of smaller thrust segments have been suggested where thrusts cut turbidite sequences in the Alps of SE France (Butler and McCaffrey, 2004, p.920). Slip along the thrust ramp may 'leak' into adjacent parts of the multilayer to create a series of smaller displacement thrusts (Butler and McCaffrey, 2004, p.920). This proposed behaviour is similar to smaller thrusts seen adjacent to larger ramps in the Zin case study. The displacement profiles vary where the thrusts cut detrital marker layers or pre-existing thrusts in the footwall (Fig. 9g–j), suggesting that competency contrast influenced fault propagation and geometries (e.g. Teixell and Koyi, 2003: Ferrill et al., 2016). In summary, this first use of D-D plots to analyse overstep thrust sequences cutting unlithified sediments demonstrates that displacement patterns along thrusts are varied and may initiate in the hangingwall above the basal detachment (e.g. Fig. 7d).

9.5.2. Displacement on basal detachments

Basal detachments to MTDs within the Lisan Formation are generally developed beneath detrital units at ~1 m depth, suggesting that a mechanical control is significant (e.g. Alsop et al., 2017a, b). Fold geometry (e.g. Fig. 8g) with 'cusps' of aragonite pointing into this detrital layer indicates that it is more competent, as do studies of buckled detrital layers elsewhere in the Lisan Formation (e.g. Alsop et al., 2017a, b). The mechanical heterogeneity displayed by the dark green marker layer within the present study, coupled with potential increases in pore pressure if the detrital unit acted as a 'seal' to the underlying aragonite, may have contributed to it being an efficient detachment. Imbricates cutting the dark green layer may have locally broken the 'seal' and reduced fluid pressure thereby facilitating reduction of movement along that particular ramp and encouraging a new ramp to form further upslope. The current high fluid content (~25%) in the Lisan Formation (Arkin and Michaeli, 1986; Frydman et al., 2008) suggests that it would have been saturated at the time of deformation in the subaqueous basin setting (Alsop et al., 2017a,b,c), explaining some of the clastic dykes that cut the entire area, and smaller-scale fingers of injected sediment directly above the detachment (e.g. Fig. 7j).

Similar stratigraphic controls on basal detachments have been described from outcrops of gravity-driven fold and thrusts belts elsewhere, and also from offshore seismic data across large-scale MTDs (Frey-Martinez et al., 2006). Clay-rich units have been considered to control basal detachments within outcrops of MTDs in California (Garcia-Tortosa et al., 2011), while basal detachments interpreted from seismic data across larger offshore gravity-driven fold and thrust belts are thought to form along specific contourite deposits (Frey-Martinez et al., 2006). Extreme weakness along basal detachments is often linked to high pore fluid pressures, as proven by drilling programmes (e.g. Moore et al., 2005), with estimates of high pore fluid pressure ratios > 0.9 (Bilotti and Shaw, 2005; Morley, 2007; Morley et al., 2017, p.218). In summary, we speculate that detrital-rich units overlying basal detachments in the Lisan Formation may have acted as a 'top seal' or baffle to fluid movement, and thereby generated fluid overpressure directly beneath it along which the basal detachment then formed. Gouge developed along the basal detachment is locally injected upwards to create 'fingers' of gouge that cut the dark green detrital marker, and attests to high fluid pressures (e.g. Fig. 7j). Earthquakes along the Dead Sea fault system may have further increased overpressure leading to slope failure and seismites within the Lisan Formation (Lu et al., 2017). Local variation in fluid overpressure along the basal detachment may also ultimately lead to variations in displacement along the detachment and consequent second order flow cells (Alsop and Marco, 2014).

9.6. Which models best constrain the geometry and kinematics of MTDs?

9.6.1. Frontally confined versus frontally emergent models within MTDs

Frey-Martinez et al. (2006) originally divided MTDs into two broad groups that they termed frontally-confined and frontally emergent depending on the geometry of the downslope toe. Where MTDs have overrun and 'spilled' on top of the undeformed downslope strata to form a frontally emergent toe, the gravity-driven fold and thrust system results in thickening and consequent surface topography (Frey-Martinez et al., 2006). However, where MTDs fail to overrun the undeformed downslope strata and do not create significant topographic relief they are termed frontally confined (Frey-Martinez et al., 2006). This distinction is important as the upper thrust tips within frontally confined MTDs are broadly at the same level, and simply define a 'tabular body which is pervasively deformed by a set of closely and regularly spaced thrusts" (Frey-Martinez et al., 2006, p.591). When describing frontally confined systems, Frey-Martinez et al. (2006, p.602) note that "continued slip is accommodated downslope by additional contractional straining within the toe region" Although no mention is made of thrust sequences (overstep or break back etc.) they do highlight "impressive frontal thrust and fold belts".

Fold- and thrust-dominated MTDs within the Lisan Formation are not generally observed to overrun downslope strata, and are not therefore frontally-emergent systems as discussed by Alsop et al. (2016, p.85). Where the terminations of MTD toes are observed in the Lisan Formation, they pass downslope into upright folds that fail to override downslope strata and are therefore best described as open-ended toes that are a variant of frontally-confined MTDs (see discussion in Alsop et al., 2016 p. 85). Although the downslope leading edge of the MTD in the present study is not exposed, it is likely that frontally confined MTDs, where the undeformed downslope strata act as a buttress to continued downslope movement at the toe may encourage overstep thrust sequences, as a compressive strain wave propagates back up slope following cessation of movement at the toe (Farrell, 1984).

9.6.2. Critical taper models versus dislocation models within MTDs

Orogenic wedges and their associated thick-skinned thrust belts are essentially modelled in terms of material being driven or pushed up a gentle detachment by compressive forces acting on a buttress from behind during collisional tectonics (the 'critical taper' model of Davis et al., 1983; Dahlen, 1990; Koyi, 1995). Conversely, MTDs are interpreted in terms of downslope-directed gravitational slope failure that induces upslope extension and downslope contraction resulting in thin-skinned fold and thrust systems (the dislocation model of Farrell, 1984). If any 'buttress' exists, it is considered to be the undeformed strata in front of the translating MTD (section 9.6.1.). While these two scenarios are clearly distinct, the downslope contractional portions of MTDs could be considered in terms of critical taper mechanics.

Within the critical taper model, extension is generally considered a consequence of a thickened wedge attempting to restore stability by reducing its thickness and taper angle. Conversely, within the dislocation model of Farrell (1984), contraction at the downslope toe is broadly balanced by extension at the upslope head, so that extension is considered a consequence of accelerating flow during translation of the slump (Alsop and Marco, 2014). If secondary flow cells develop at smaller scales, then simultaneous movement of individual flow cells may result in a range of overprinting relationships incorporating contraction and extension within the toe region (see Alsop and Marco, 2014).

Previous analysis of critical tapers calculated from wedge thicknesses over distances of ~500 m indicates negligible taper angles of between 0.19° and 0.38° for MTDs elsewhere in the Lisan Formation (Alsop et al., 2017a). These values are an order of magnitude less than taper angles from large-scale accretionary wedges that have calculated angles of 4.7° (e.g. Yang et al. in press). The lack of significant taper angles within MTDs of the Lisan Formation was attributed to very weak

sediments that form the fold and thrust system, together with low-friction basal detachments that follow weak bedding planes, and higher density brines that overlie the failed sediment mass (Alsop et al., 2017a). Although thrusts duplicate stratigraphy, the MTD's of the Lisan Formation lack evidence of a build-up of topography or erosion during thrusting, although truncation may occur immediately afterwards during deposition of the sedimentary 'cap'. Given the rapidity of slope failure, very little time exists for adjustments to wedge morphology before deposition of this cap that may have lasted just hours or days (Alsop et al., 2016). Within the case study, upper thrust tips terminate at the same level, while the basal detachment maintains its position directly beneath the dark green detrital layer. Consequently, no evidence exists for thickening and surface uplift, or of the basal detachment cutting deeper in a process of 'underplating' to actually create a wedge or critical taper. Our study therefore supports the findings of Frey-Martinez (2006, p.591) who noted that frontally-confined MTDs "do not define a critical wedge". The critical taper model may not therefore be the most suitable model in this case, although factors that influence the stability and geometry of a series of thrust imbricates, such as the thickness of the deformed sequence, friction along the basal detachment and 'strength' of the sediments may all clearly influence the resulting geometry.

9.6.3. Models and controls on thrust spacing within MTDs

Within the present study, the thickness of the deformed sequence is 0.8 m and the average thrust spacing along the disused track is 4.66 m (Fig. 3). These values yield a thickness to thrust spacing ratio (see Liu and Dixon, 1995) of 1:5.8 that is broadly similar to the 1:5 ratio calculated for thrusts elsewhere in the Lisan Formation (Alsop et al., 2017a,b,c), and also from seismic analysis of larger-scale offshore gravity-driven fold and thrust belts (e.g. Butler and Paton, 2010; Morley et al., 2017, p.180). Morley et al. (2017 p.175) indicated that the thrust thickness to ramp spacing ratio in major orogenic thrust belts ranges between 1:1 and 1:5, with thrust spacing increasing with thrust sheet thickness. The slightly higher ratio in the case study (1:5.8) may reflect a weaker basal detachment relative to the strength of the sediment potentially created by trapped pore fluids beneath the green detrital marker (see also Mulugeta, 1988; Morley et al., 2017, p.176).

Physical modelling indicates that a decrease in friction along the basal detachment also increases the number of backthrusts, with the initial ramp angle of backthrusts (35°–40°) and forethrusts (25°–30°) appearing to be unaffected by the basal friction (Liu et al., 1992). These angles, together with the number of backthrusts in the present study support the interpretation of a weak basal detachment. In addition, analogue modelling by Deng et al. (2017) suggests that greater displacement velocities along basal detachments also result in increased fault spacing and a greater number of backthrusts. Rates of displacement may be important given that slope failures and resulting fold and thrust systems within the Lisan Formation are considered to form within a matter of hours or days before deposition of the overlying sedimentary cap out of suspension (Alsop et al., 2016). It would appear that within the case study, thrust spacing, together with forethrust and backthrust geometries are broadly consistent with both analogue models and analysis of larger scale fold and thrust systems developed in accretionary complexes and orogenic belts.

In summary, the critical taper model may be most applicable to frontally emergent MTDs that overrun the downslope area and create new topography, whereas it is less suitable for frontally confined MTDs. In this case, the MTD cannot be defined as a critical taper as the basal detachment remains at the same horizon, while thrusts do not propagate to higher levels meaning that the top of the MTD lacks topography and remains at the same level, with no wedge or taper actually created (Frey-Martinez et al., 2006 p.591). Studies of MTDs within the Lisan Formation, including the present case study, are interpreted in terms of frontally confined or open-ended MTDs and are best interpreted in terms of dislocation models where contraction and extension are linked to variable displacement along the underlying basal detachment. However, aspects of the critical taper model, including the relationship between thrust spacing and thickness of the deformed sequence, seem to have similar ratios to those recorded elsewhere in orogenic belts and accretionary complexes. Friction along the basal detachment may control overall geometries and development of back thrusts, while the position of the initial toe thrust may be influenced by early buckle folding or detrital facies variation (see discussion in Alsop et al., 2016).

10. Conclusions

In summary, our study forms the first detailed analysis of overstep thrust sequences developed in a gravity-driven fold and thrust belt, and provides a range of criteria to distinguish different thrust sequences. Cross-cutting relationships whereby folds and thrusts are truncated by overlying thrusts are the most straightforward principle to determine overstep thrust sequences. In addition, loading and deflection of underlying thrusts by overthrust sheets, and structural inheritance relating to the position of the underlying thrust ramp, may control the geometry of the overlying and younger thrust sheet within overstep thrust sequences. We identify, four possible scenarios for the interaction of forethrusts and backthrusts in piggyback and overstep thrust sequences. Overstep thrust sequences are marked by backthrusts being truncated and displaced by overlying forethrusts, while older forethrusts may be carried and rotated in the hangingwall of younger backthrusts.

Within MTDs, overstep thrust sequences get younger in a direction opposite to the overall downslope thrust vergence, and are traditionally thought to develop at a 'late stage' due to cessation of movement at the downslope toe. In the present case study, the overstep thrust sequence does not overprint any earlier structures, and is therefore considered to form because of a deceleration of flow during actual translation of the MTD. Synchronous thrusting within this overstep sequence is supported by: a) systematic increases in displacement across older imbricates in the thrust system, whereby older thrusts continue to move and therefore accumulate the greatest displacement; b) bridging 'short-cut' faults that develop below folded detachments; and c) backthrusts truncated by forethrusts that become immediately inactive and therefore display less displacement during synchronous thrusting. In detail, displacement-distance plots show that displacement may increase up the thrust ramp, suggesting that thrusts initiated in the hangingwall of the basal detachment during overstep thrusting. Displacement patterns are in addition influenced by a) the position of detrital marker horizons, b) the location of older (and truncated) thrusts in the footwall.

Frontally confined MTDs may display overstep thrust sequences developed from a basal detachment that maintains the same stratigraphic horizon. Thrusts terminate at the same upper level meaning that the MTD lacks topography and does not define a critical taper. Thrust sheet thickness to ramp spacing ratios are however similar to those recorded in accretionary complexes and orogenic belts, and frontally confined MTDs may therefore be better interpreted using models of dislocation and thrust ramp spacing along the basal detachment. Although the detailed relationships observed in this study are clearly below the limits of seismic resolution, they do provide a template for the types and styles of structural interaction that may be generated within MTDs. The overall displacement paths formed across imbricates during synchronous thrusting may be resolvable in seismic sections, and therefore represents a viable test of synchronous thrusting within large-scale MTDs.

Acknowledgements

RW was supported by the Israel Science Foundation (ISF grant No. 868/17). SM acknowledges the Israel Science Foundation (ISF grant No. 1436/14) and the Ministry of National Infrastructures, Energy and Water Resources (grant # 214-17-027). We would like to thank Chris Morley and an anonymous referee for careful and constructive reviews,

together with Bill Dunne, for efficient editorial handling of the manuscript.

References

Agnon, A., Migowski, C., Marco, S., 2006. Intraclast breccia layers in laminated sequences: recorders of paleo-earthquakes, in Enzel, Y., Agnon, A., and Stein, M., eds., New Frontiers in Dead Sea Paleoenvironmental Research, Geological Society of America Special Publication, p. 195–214.

Alsop, G.I., Marco, S., 2011. Soft-sediment deformation within seismogenic slumps of the Dead Sea Basin. J. Struct. Geol. 33, 433–457.

Alsop, G.I., Marco, S., 2012a. A large-scale radial pattern of seismogenic slumping towards the Dead Sea Basin. J. Geol. Soc. 169, 99–110.

Alsop, G.I., Marco, S., 2012b. Tsunami and seiche-triggered deformation within offshore sediments. Sediment. Geol. 261, 90–107.

Alsop, G.I., Marco, S., 2013. Seismogenic slump folds formed by gravity-driven tectonics down a negligible subaqueous slope. Tectonophysics 605, 48–69.

Alsop, G.I., Marco, S., 2014. Fold and fabric relationships in temporally and spatially evolving slump systems: a multi-cell flow model. J. Struct. Geol. 63, 27–49.

Alsop, G.I., Marco, S., Weinberger, R., Levi, T., 2016. Sedimentary and structural controls on seismogenic slumping within mass transport deposits from the Dead Sea Basin. Sediment. Geol. 344, 71–90.

Alsop, G.I., Marco, S., Levi, T., Weinberger, R., 2017a. Fold and thrust systems in mass transport deposits. J. Struct. Geol. 94, 98–115.

Alsop, G.I., Marco, S., Weinberger, R., Levi, T., 2017b. Upslope-verging back thrusts developed during downslope-directed slumping of mass transport deposits. J. Struct. Geol. 100, 45–61.

Alsop, G.I., Weinberger, R., Marco, S., Levi, T., 2017c. Identifying soft-sediment deformation in rocks. J. Struct. Geol. http://dx.doi.org/10.1016/j.jsg.2017.09.001.

Arkin, Y., Michaeli, L., 1986. The significance of shear strength in the deformation of laminated sediments in the Dead Sea area. Isr. J. Earth Sci. 35, 61–72.

Bartov, Y., Steinitz, G., Eyal, M., Eyal, Y., 1980. Sinistral movement along the Gulf of Aqaba - its age and relation to the opening of the red Sea. Nature 285, 220–221.

Basilone, L., 2017. Seismogenic rotational slumps and translational glides in pelagic deep-water carbonates. Upper Tithonian-Berriasian of Southern Tethyan margin (W Sicily, Italy). Sediment. Geol. 356, 1–14.

Begin, Z.B., Ehrlich, A., Nathan, Y., 1974, Lake Lisan, the Pleistocene precursor of the Dead Sea: Geological survey of Israel Bulletin, 63, p. 30.

Bilotti, F., Shaw, J.H., 2005. Deep-water Niger Delta fold and thrust belt modeled as a critical taper wedge: the influence of elevated basal fluid pressure on structural styles. AAPG (Am. Assoc. Pet. Geol.) Bull. 89, 1475–1491.

Boyer, S.E. 1992. Geometric evidence for synchronous thrusting in the southern Alberta and northwest Montana thrust belts. In: McClay, K. (Editor), Thrust Tectonics. Chapman and Hall. London. p. 377–390.

Boyer, S.E., Elliot, D., 1982. Thrust systems. AAPG (Am. Assoc. Pet. Geol.) Bull. 66, 1196–1230.

Bull, S., Cartwright, J., Huuse, M., 2009. A review of kinematic indicators from mass-transport complexes using 3D seismic data. Mar. Petrol. Geol. 26, 1132–1151.

Butler, R.W.H., 1982. The terminology of structures in thrust belts. J. Struct. Geol. 4, 239–245.

Butler, R.W.H., 1987. Thrust sequences. J. Geol. Soc. Lond. 144, 619–634.

Butler, R.W.H., 2004. The nature of 'roof thrusts' in the Moine Thrust Belt, NW Scotland: implications for the structural evolution of thrust belts. J. Geol. Soc. Lond. 161, 1–11.

Butler, R.W.H., Coward, M.P., 1984. Geological constraints, structural evolution and deep geology of the Northwest Scottish Caledonides. Tectonics 3, 347–365.

Butler, R.W.H., McCaffrey, W.D., 2004. Nature of thrust zones in deep water sand-shale sequences: outcrop examples from the Champsaur sandstones of SE France. Mar. Petrol. Geol. 21, 911–921.

Butler, R.W.H., Paton, D.A., 2010. Evaluating lateral compaction in deepwater fold and thrust belts: How much are we missing from "nature's sandbox"? GSA Today (Geol. Soc. Am.) 20, 4–10. http://dx.doi.org/10.1130/GSATG77A.1.

Chapman, T.J., Williams, G.D., 1984. Displacement-distance methods in the analysis of fold-thrust structures and linked-fault systems. J. Geol. Soc. 141, 121–128.

Cooper, M.A. 1981. The internal geometry of nappes: criteria for models of emplacement. In: McClay K.R., Price N.J. (eds.) Thrust and Nappe Tectonics. Special Publication of the Geological Society of London vol. 9, 225–234.

Coward, M.P., 1985. The thrust structures of southern Assynt, Moine thrust zone. Geol. Mag. 122, 595–607.

Cruciani, F., Barchi, M.R., Koyi, H.A., Porreca, M., 2017. Kinematic evolution of a regional-scale gravity-driven deepwater fold-and-thrust belt: the Lamu Basin case-history (East Africa). Tectonophysics 712–713, 30–44.

Dahlen, F.A., 1990. Critical taper model of fold- and thrust- belts and accretionary wedges. Annu. Rev. Earth Planet Sci. 18, 55–99.

Davis, D., Suppe, J., Dahlen, F.A., 1983. Mechanics of fold-and-thrust belts and accretionary wedges. J. Geophys. Res. 88 (B2), 1153–1172.

Dahlstrom, C.D.A., 1970. Structural geology in the eastern margin of the Canadian Rocky Mountains. Bull. Can. Petrol. Geol. 18, 332–406.

Deng, B., Jiang, L., Zhao, G., Huang, R., Wang, Y., Liu, S., 2017. Insights into the velocity-dependent geometry and internal strain in accretionary wedges from analogue models. Geol. Mag. http://dx.doi.org/10.1017/S0016756816001266.

de Vera, J., Granado, P., McClay, K., 2010. Structural evolution of the Orange Basin gravity-driven system, offshore Namibia. Mar. Petrol. Geol. 27, 223–237.

El-Isa, Z.H., Mustafa, H., 1986. Earthquake deformations in the Lisan deposits and seismotectonic implications. Geophys. J. Roy. Astron. Soc. 86, 413–424.

Elliot, D., 1976. The energy balance and deformation mechanisms of thrust sheets. Philos. Trans. R. Soc. London, Ser. A 283, 289–312.

Elliot, D., Johnson, M.R.W., 1980. Structural evolution in the northern part of the moine thrust belt of NW scotland. Transactions of the Royal society of Edinburgh. Earth Sci. 71B, 69–96.

Ellis, M.A., Dunlap, W.J., 1988. Displacement variation along thrust faults: implications for the development of large faults. J. Struct. Geol. 10, 183–192.

Farrell, S.G., 1984. A dislocation model applied to slump structures, Ainsa Basin, South Central Pyrenees. J. Struct. Geol. 6, 727–736.

Ferrill, D.A., Morris, A.P., Wigginton, S.S., Smart, K.J., McGinnis, R.N., Lehrmann, D., 2016. Deciphering thrust fault nucleation and propagation and the importance of footwall synclines. J. Struct. Geol. 85, 1–11.

Fossen, H. 2016. Structural Geology. second ed.. Cambridge University Press, Cambridge, UK, p.510.

Frey-Martinez, J., Cartwright, J., Hall, B., 2005. 3D seismic interpretation of slump complexes: examples from the continental margin of Israel. Basin Res. 17, 83–108.

Frey-Martinez, J., Cartwright, J., James, D., 2006. Frontally confined versus frontally emergent submarine landslides: a 3D seismic characterisation. Mar. Petrol. Geol. 23, 585–604.

Frydman, S., Charrach, J., Goretsky, I., 2008. Geotechnical properties of evaporite soils of the Dead Sea area. Eng. Geol. 101, 236–244.

Garcia-Tortosa, F.J., Alfaro, P., Gibert, L., Scott, G., 2011. Seismically induced slump on an extremely gentle slope ($< 1^{\circ}$) of the Pleistocene Tecopa paleolake (California). Geology 39, 1055–1058.

Garfunkel, Z., 1981. Internal structure of the Dead Sea leaky transform (rift) in relation to plate kinematics. Tectonophysics 80, 81–108.

Garfunkel, Z., Ben-Avraham, Z., 1996. The structure of the Dead Sea basin. Tectonophysics 26, 155–176.

Gibert, L., Sanz de Galdeano, C., Alfaro, P., Scott, G., Lopez Garrido, A.C., 2005. Seismic-induced slump in early Pleistocene deltaic deposits of the Baza basin (SE Spain). Sediment. Geol. 179, 279–294.

Haase-Schramm, A., Goldstein, S.L., Stein, M., 2004. U-Th dating of Lake Lisan aragonite (late Pleistocene Dead Sea) and implications for glacial East Mediterranean climate change. Geochem. Cosmochim. Acta 68, 985–1005.

Haliva-Cohen, A., Stein, M., Goldstein, S.L., Sandler, A., Starinsky, A., 2012. Sources and transport routes of fine detritus material to the late quaternary Dead Sea Basin. Quat. Sci. Rev. 50, 55–70.

Hedlund, C.A., 1997. Fault-propagation, ductile strain, and displacement-distance relationships. J. Struct. Geol. 19, 249–256.

Ireland, M.T., Davies, R.J., Goulty, N.R., Moy, D.J., 2011. Thick slides dominated by regular-wavelength folds and thrusts in biosiliceous sediments on the Vema Dome offshore of Norway. Mar. Geol. 289, 34–45.

Jolly, B.A., Lonergan, L., Whittaker, A.C., 2016. Growth history of fault-related folds and interaction with seabed channels in the toe-thrust region of the deep-water Niger delta. Mar. Petrol. Geol. 70, 58–76.

Kim, Y.S., Sanderson, D.J., 2005. The relationship between displacement and length of faults. Earth Sci. Rev. 68, 317–334.

Korneva, I., Tondi, E., Jablonska, D., Di Celma, C., Alsop, I., Agosta, F., 2016. Distinguishing tectonically- and gravity-driven synsedimentary deformation structures along the Apulian platform margin (Gargano Promontory, southern Italy). Mar. Petrol. Geol. 73, 479–491.

Koyi, H., 1995. Mode of internal deformation in sand wedges. J. Struct. Geol. 17, 293–300.

Liu, H. McClay, K.R., Powell, D. 1992. Physical models of thrust wedges. In: McClay, K.R. (Editor) Thrust Tectonics. Chapman and Hall, London. P. 71–81.

Liu, S., Dixon, J.M., 1995. Localization of duplex thrust-ramps by buckling: analog and numerical modelling. J. Struct. Geol. 17, 875–886.

Lu, Y., Waldmann, N., Alsop, G.I., Marco, S., 2017. Interpreting soft sediment deformation and mass transport deposits as seismites in the Dead Sea depocentre. J. Geophys. Res.: Solid Earth 122 (10), 8305–8325. http://dx.doi.org/10.1002/2017JB014342.

Lucente, C.C., Pini, G.A., 2003. Anatomy and emplacement mechanism of a large submarine slide within a Miocene foredeep in the northern Appenines, Italy: a field perspective. Am. J. Sci. 303, 565–602.

Marco, S., Agnon, A., 1995. Prehistoric earthquake deformations near Masada, Dead Sea graben. Geology 23, 695–698.

Marco, S., Kagan, E.J. 2014. Deformed sediments in the Dead Sea drill core: a long term palaeoseismic record. EGU General Assembly Conference Abstracts, vol. 16, 4375. (Vienna).

Marco, S., Stein, M., Agnon, A., Ron, H., 1996. Long term earthquake clustering: a 50,000 year paleoseismic record in the Dead Sea Graben. J. Geophys. Res. 101, 6179–6192.

Martinsen, O.J., Bakken, B., 1990. Extensional and compressional zones in slumps and slides in the namurian of county Claire, Eire. J. Geol. Soc. Lond. 147, 153–164.

McClay, K.R., 1992. Glossary of thrust tectonic terms. In: McClay, K.R. (Editor) Thrust Tectonics. Chapman and Hall, London. P. 419–433.

Moore, G.F., Mikada, H., Moore, C.J., Becker, K., Taira, A. 2005. 1. Legs 190 and 196 synthesis: deformation and fluid flow processes in the Nankai Trough accretionary prism. In: Mikada H., Moore G.F., Taira A., Becker K., Moore J.C., Klaus, A. (Eds.), Proc. ODP Scientific Results 190/196. pp.1-26.

Morley, C.K., 1988. Out-of-sequence thrusts. Tectonics 7, 539–561.

Morley, C.K., 2007. Interaction between critical wedge geometry and sediment supply in a deepwater fold belt, NW Borneo. Geology 35, 139–142.

Morley, C.K., King, R., Hillis, R., Tingay, M., Backe, G., 2011. Deepwater fold and thrust belt classification, tectonics, structure and hydrocarbon prospectivity: a review. Earth Sci. Rev. 104, 41–91.

Morley, C.K., von Hagke, C., Hansberry, R.L., Collins, A.S., Kanitpanyacharoen, W., King, R., 2017. Review of major shale-dominated detachment and thrust characteristics in

the diagenetic zone: Part I, meso- and macro-scopic scale. Earth Sci. Rev. 173, 168–228.
Mulugeta, G., 1988. Modelling the geometry of Coulomb thrust wedges. J. Struct. Geol. 10, 847–859.
Muraoka, H., Kamata, H., 1983. Displacement distribution along minor fault traces. J. Struct. Geol. 5, 483–495.
Nuriel, P., Weinberger, R., Kylander-Clark, A.R.C., Hacker, B.R., Cradock, J.P., 2017. The onset of the Dead Sea transform based on calcite age-strain analyses. Geology 45, 587–590.
Ortner, H., Kilian, S., 2016. Sediment creep on slopes in pelagic limestones: upper Jurassic of northern Calcareous Alps, Austria. Sediment. Geol. 344, 350–363.
Park, R.G. 2013. Foundations of Structural Geology. Routledge, Oxford, UK. pp. 214. ISBN-1136784357.
Peacock, D.C.P., Sanderson, D.J., 1996. Effects of propagation rate on displacement variations along faults. J. Struct. Geol. 18, 311–320.
Peel, F.J., 2014. The engines of gravity-driven movement on passive margins: quantifying the relative contribution of spreading vs. gravity sliding mechanisms. Tectonophysics 633, 126–142.
Prasad, S., Negendank, J.F.W., Stein, M., 2009. Varve counting reveals high resolution radiocarbon reservoir age variations in palaeolake Lisan. J. Quat. Sci. 24, 690–696.
Reis, A.T., Araújo, E., Silva, C.G., Cruz, A.M., Gorini, C., Droz, L., Migeon, S., Perovano, R., King, I., Bache, F., 2016. Effects of a regional décollement level for gravity tectonics on late Neogene to recent large-scale slope instabilities in the Foz do Amazonas Basin, Brazil. Mar. Petrol. Geol. 75, 29–52.
Scarselli, N., McClay, K., Elders, C., 2016. Seismic geomorphology of Cretaceous mega-slides offshore Namibia (Orange Basin): insights into segmentation and degradation of gravity-driven linked systems. Mar. Petrol. Geol. 75, 151–180.
Sharman, G.R., Graham, S.A., Masalimova, L.U., Shumaker, L.E., King, P.R., 2015. Spatial patterns of deformation and palaeoslope estimation within the marginal and central portions of a basin-floor mass-transport deposit, Taranaki Basin, New Zealand. Geosphere 11, 266–306.
Smit, J., Brun, J.-P., Fort, X., Cloetingh, S., Ben-Avraham, Z., 2008. Salt tectonics in pull-apart basins with application to the Dead Sea Basin. Tectonophysics 449, 1–16.
Sneh, A., Weinberger, R. 2014. Major Structures of Israel and Environs, Scale 1:50,000. Israel Geological Survey, Jerusalem.
Sobiesiak, M., Alsop, G.I., Kneller, B.C., Milana, J.P., 2017. Sub-seismic scale folding and thrusting within an exposed mass transport deposit: a case study from NW Argentina. J. Struct. Geol. 96, 176–191.
Strachan, L.J., 2002. Slump-initiated and controlled syndepositional sandstone re-mobilization; an example from the Namurian of County Clare, Ireland. Sedimentology 49, 25–41.
Strachan, L.J., 2008. Flow transformations in slumps: a case study from the Waitemata Basin, New Zealand. Sedimentology 55, 1311–1332.
Strachan, L.J., Alsop, G.I., 2006. Slump folds as estimators of palaeoslope: a case study from the Fisherstreet Slump of County Clare, Ireland. Basin Res. 18, 451–470.
Teixell, A., Koyi, H.A., 2003. Experimental and field study of the effects of lithological contrasts on thrust-related deformation. Tectonics 22, 1054. http://dx.doi.org/10.1029/2002TC001407.
Totake, Y., Butler, R.W.H., Bond, C.E., Aziz, A., 2017. Analyzing structural variations along strike in a deep-water thrust belt. J. Struct. Geol. http://dx.doi.org/10.1016/j.jsg 2017.06.007.
Weinberger, R., Levi, T., Alsop, G.I., Eyal, Y., 2016. Coseismic horizontal slip revealed by sheared clastic dikes in the Dead Sea basin. Geol. Soc. Am. Bull. 128, 1193–1206.
Weinberger, R., Levi, T., Alsop, G.I., Marco, S., 2017. Kinematics of mass transport deposits revealed by magnetic fabrics. Geophys. Res. Lett. 44, 7743–7749.
Williams, G., Chapman, T., 1983. Strains developed in the hangingwall of thrusts due to their slip/propagation rate: a dislocation model. J. Struct. Geol. 5, 563–571.
Woodcock, N.H., 1976a. Ludlow series slumps and turbidites and the form of the Montgomery trough, Powys, Wales. Proc. Geol. Assoc. 87, 169–182.
Woodcock, N.H., 1976b. Structural style in slump sheets: Ludlow series, Powys, Wales. J. Geol. Soc. Lond. 132, 399–415.
Woodcock, N.H., 1979. The use of slump structures as palaeoslope orientation estimators. Sedimentology 26, 83–99.
Yang, C.M., Dong, J.J., Hsieh, Y.L., Liu, H.H., Cheng, L.L., 2018. Non-linear critical taper model and determination of accretionary wedge strength. Tectonophysics. http://dx.doi.org/10.1016/j.tecto.2016.04.026. (in press).